The nucleon axial charge g_A from lattice QCD

Chris Bouchard
University of Glasgow

work with 

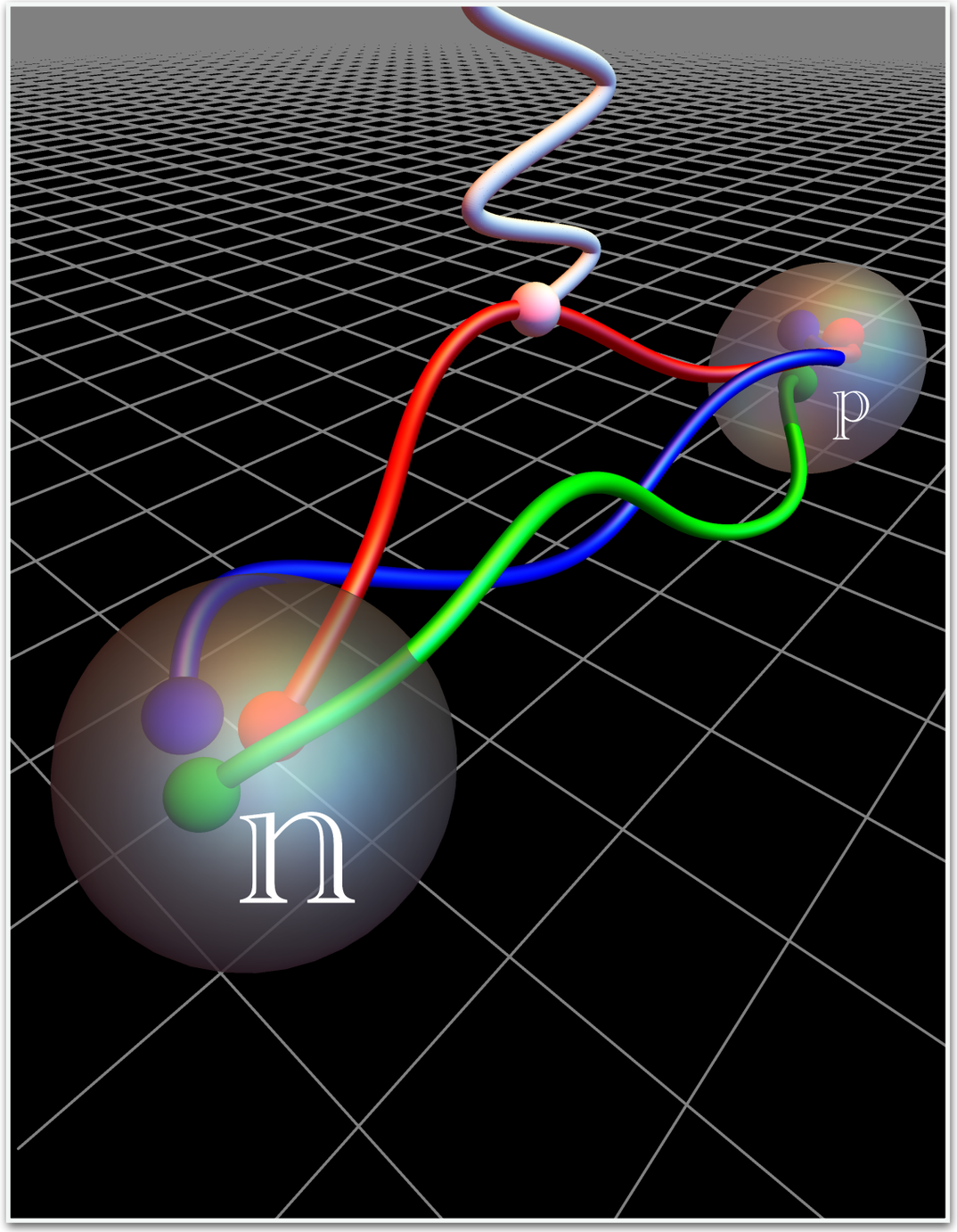

- Introduction
  - g_A and its phenomenology
  - experiment vs theory
- CalLat '18 calculation
  - simulation
    - HISQ 2+1+1 gauge fields
    - gradient flow smearing with Möbius DW valence quarks
  - Feynman-Hellmann Theorem inspired approach to correlators
  - renormalization; chiral, continuum, and infinite volume extrapolation
- Summary and outlook

g_A and its phenomenology

- quark flavor-changing transition in nucleon

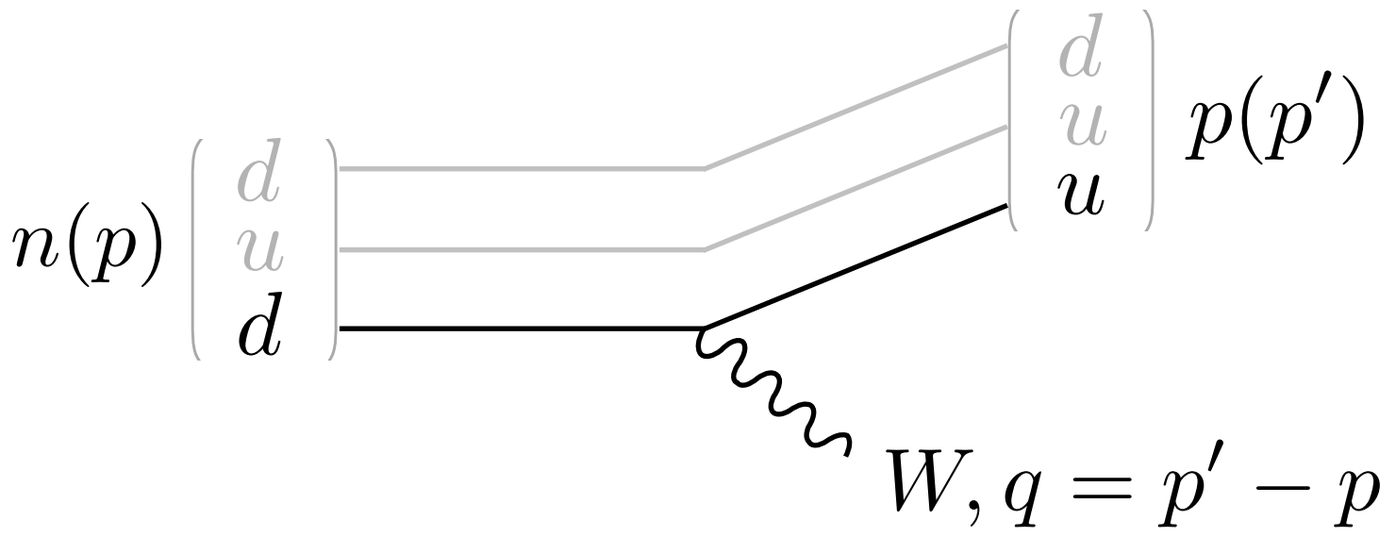

$$\langle p(p')|W_\mu|n(p)\rangle = \bar{u}^{(p)}(p')\Big[\gamma_\mu F_1(q^2) + i\sigma_{\mu\nu}\frac{q^\nu}{2M_N}F_2(q^2) + \frac{q_\mu}{M_N}F_S(q^2)$$
$$- \gamma_\mu\gamma_5 F_A(q^2) + \gamma_5\frac{q_\mu}{M_N}F_P(q^2) + \gamma_5\frac{(p'+p)_\mu}{M_N}F_T(q^2)\Big]u^{(n)}(p)$$

Dirac, Pauli, induced scalar, axial-vector, induced pseudoscalar, induced tensor

where $M_N = (M_p + M_n)/2$.

g_A and its phenomenology

$$\langle p(p')|W_\mu|n(p)\rangle = \bar{u}^{(p)}(p')\Big[\gamma_\mu F_1(q^2) + i\sigma_{\mu\nu}\frac{q^\nu}{2M_N}F_2(q^2) + \frac{q_\mu}{M_N}F_S(q^2)$$
$$- \gamma_\mu\gamma_5 F_A(q^2) + \gamma_5\frac{q_\mu}{M_N}F_P(q^2) + \gamma_5\frac{(p'+p)_\mu}{M_N}F_T(q^2)\Big]u^{(n)}(p)$$

$$g_A = F_A(0)$$

- fundamental property of nucleon structure
- inherently nonperturbative
- for years, considered a benchmark for LQCD
- in principle, straightforward:
  - no momenta (in isospin limit)
  - isovector (so no disconnected quark loop)
  - same mature LQCD technology as for meson form factors
- relevant to...

g_A and its phenomenology

- rate of neutron beta decay, i.e. neutron lifetime

$$\frac{1}{\tau_n} = \frac{G_F^2 g_V^2 m_e^5}{2\pi^3} |V_{\mathrm{ud}}|^2 \left[1 + \left(\frac{g_A}{g_V}\right)^2\right] f_V (1 + \mathrm{RC})$$

  - beam measurements dropped by PDG
  - more precision from LQCD required to weigh in
  - new radiative correction of $\mathcal{O}(0.4\%)$ Hayen and Severijns, 1906.09870

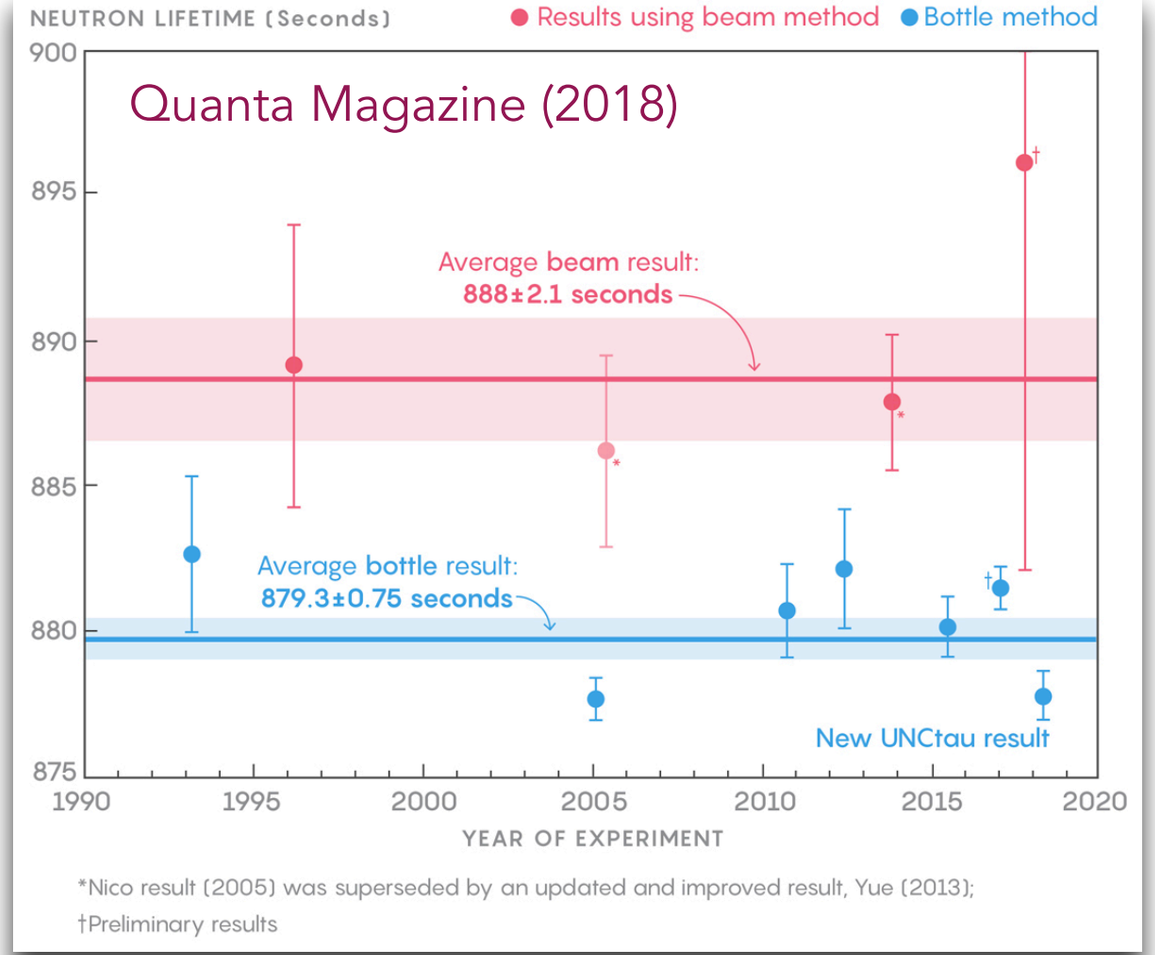

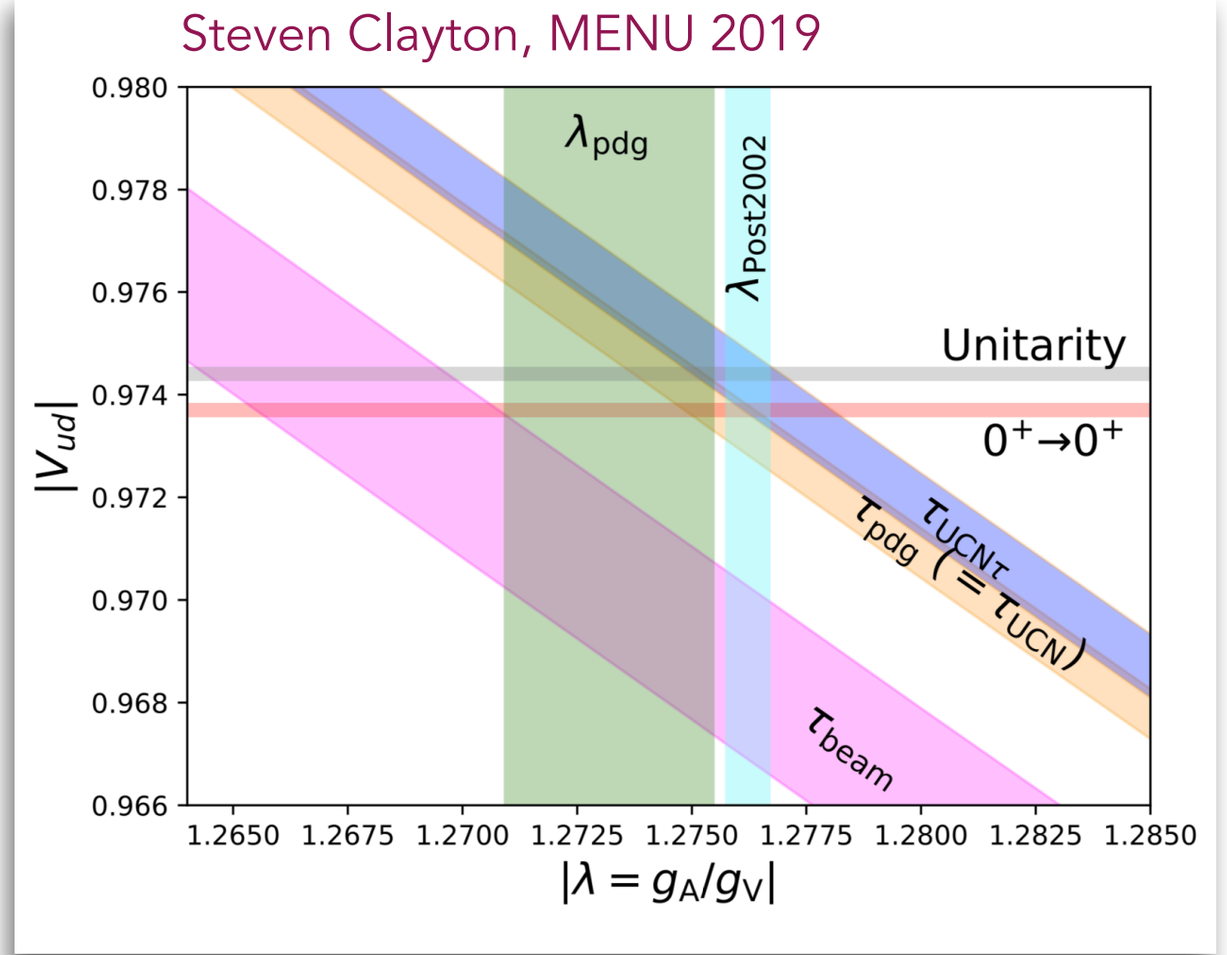

g_A and its phenomenology

- long-range N-N interaction
  - single π exchange at large distances, $\gtrsim 2$ fm
  - Goldberger-Tremain relation

$$g_{\pi NN} = g_A M_N / F_\pi$$

  - first step in nuclear EFT connecting to LQCD calculations of N-N interactions, e.g.,

McElvain and Haxton, PLB 134880 (2019)

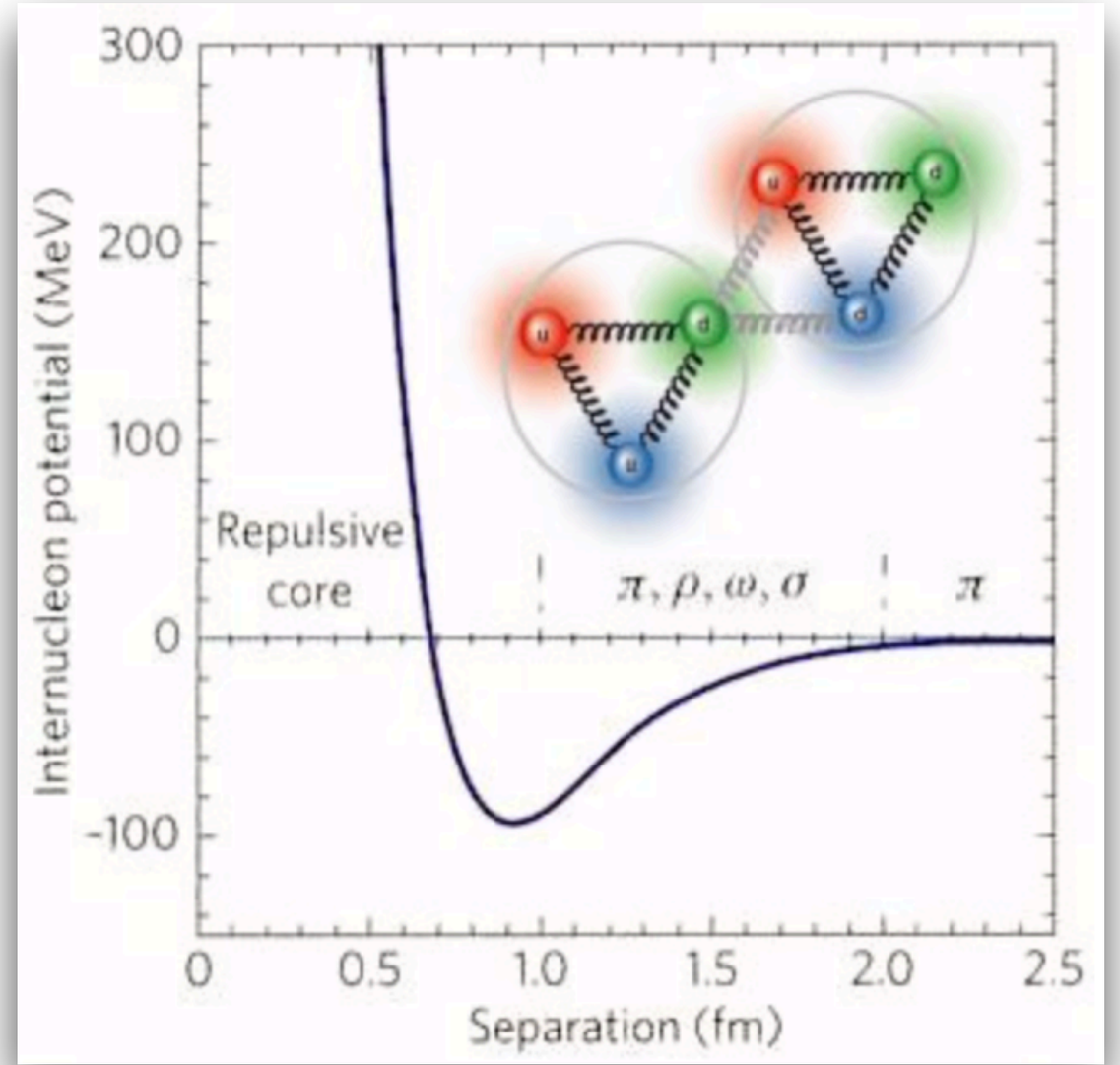

g_A and its phenomenology

- constraining new physics, e.g., RH currents

$$\left(\frac{g_A}{g_V}\right)^{\text{expt.}} = \left(\frac{g_A}{g_V}\right)^{\text{SM}} (1 - 2\mathscr{R}e\epsilon_{\text{R}})$$

  - new radiative correction of $\mathcal{O}(0.4\%)$ important here

Hayen and Severijns, 1906.09870

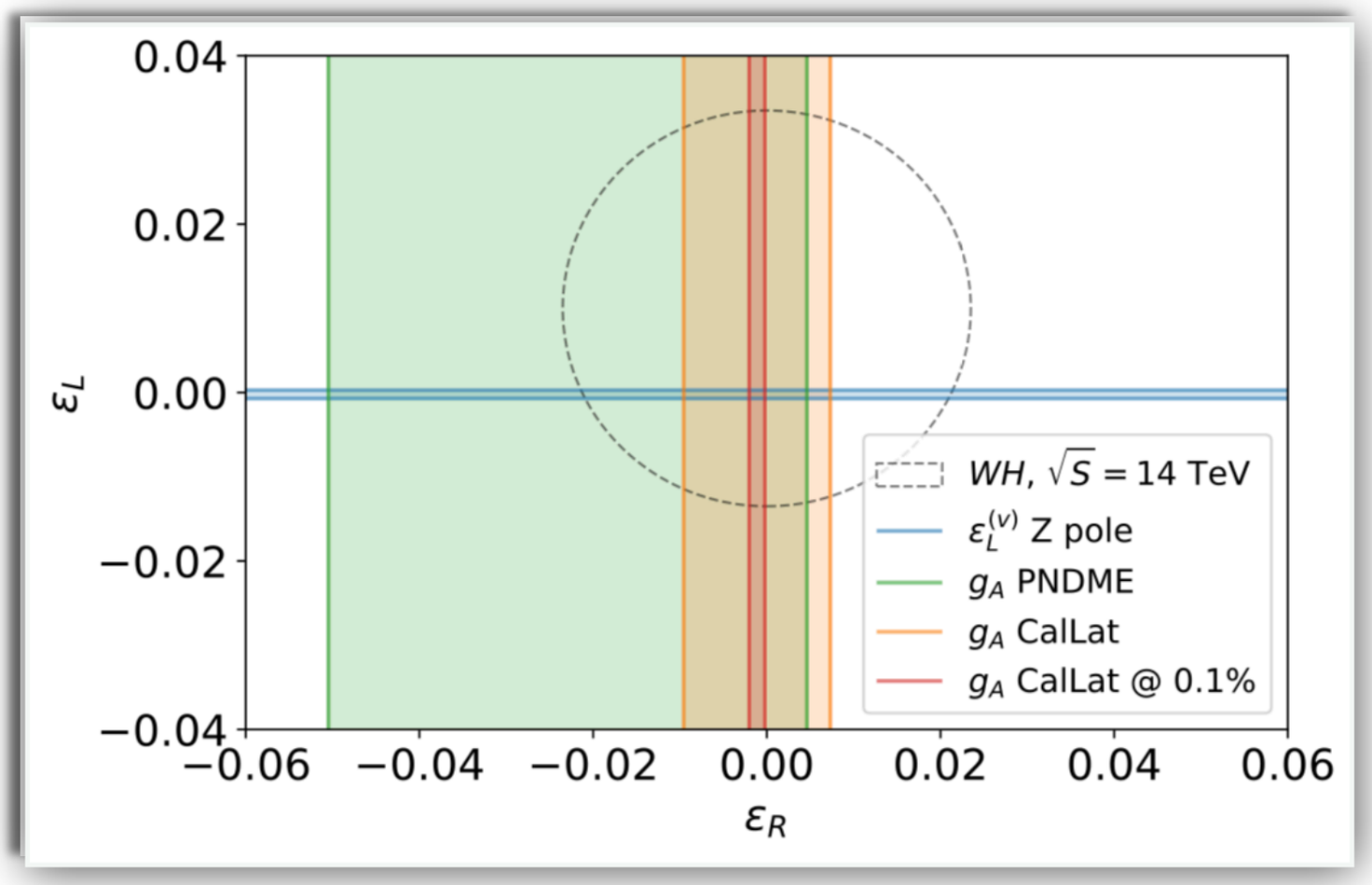

g_A and its phenomenology

- ν-nucleus interactions at small q^2
  - cross section per N for range of nuclear targets (D_2, C, Al, CF_3Br, ...)
  - QE ν-N dominates at low $E_{\bar{\nu}}$
  - several LQCD calculations underway for $F_A(q^2 \lesssim 1\ \mathrm{GeV}^2)$
  - $F_A(q^2 \lesssim 1\ \mathrm{GeV}^2)$ at 5% may allow isolation of T2K nuclear effects

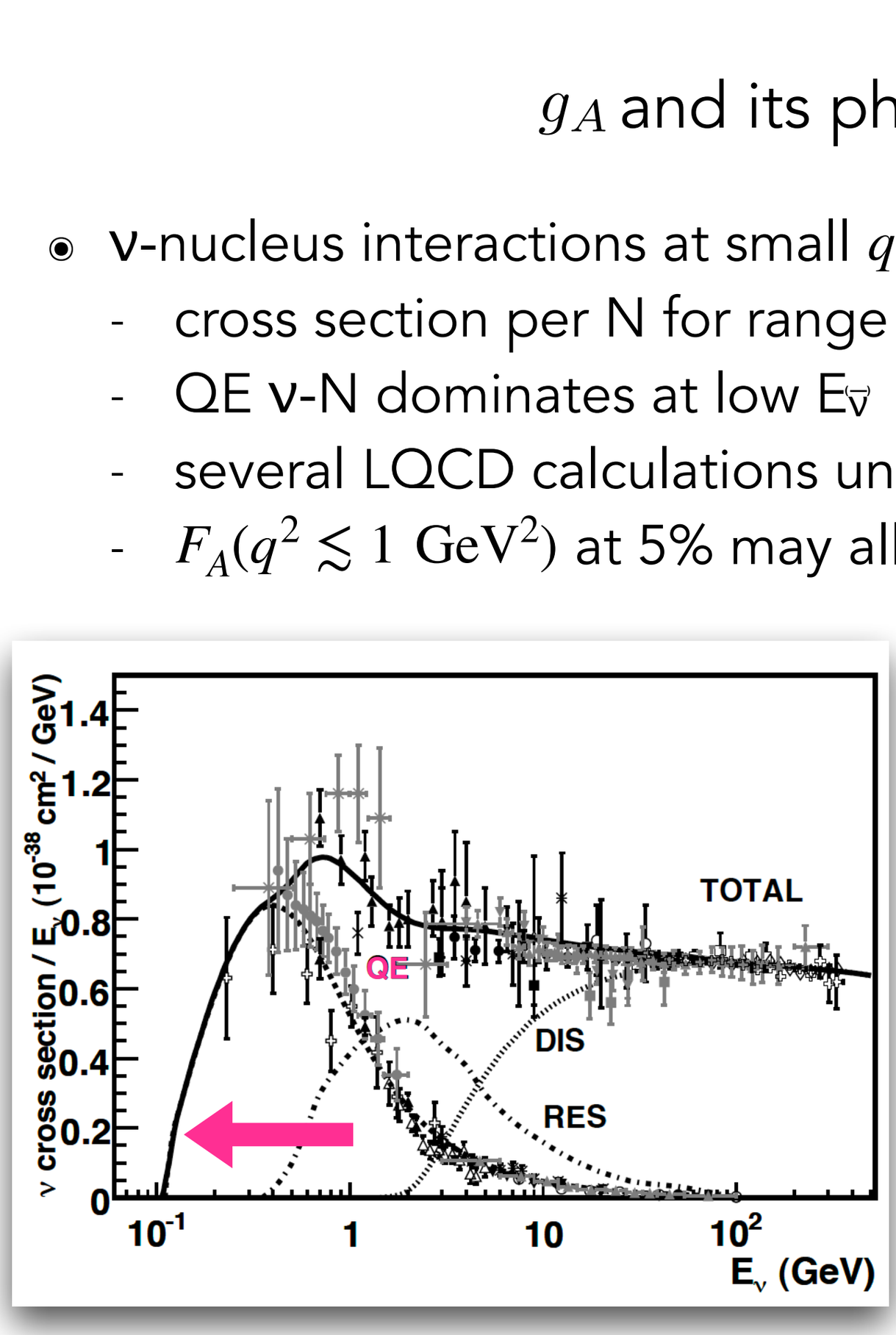

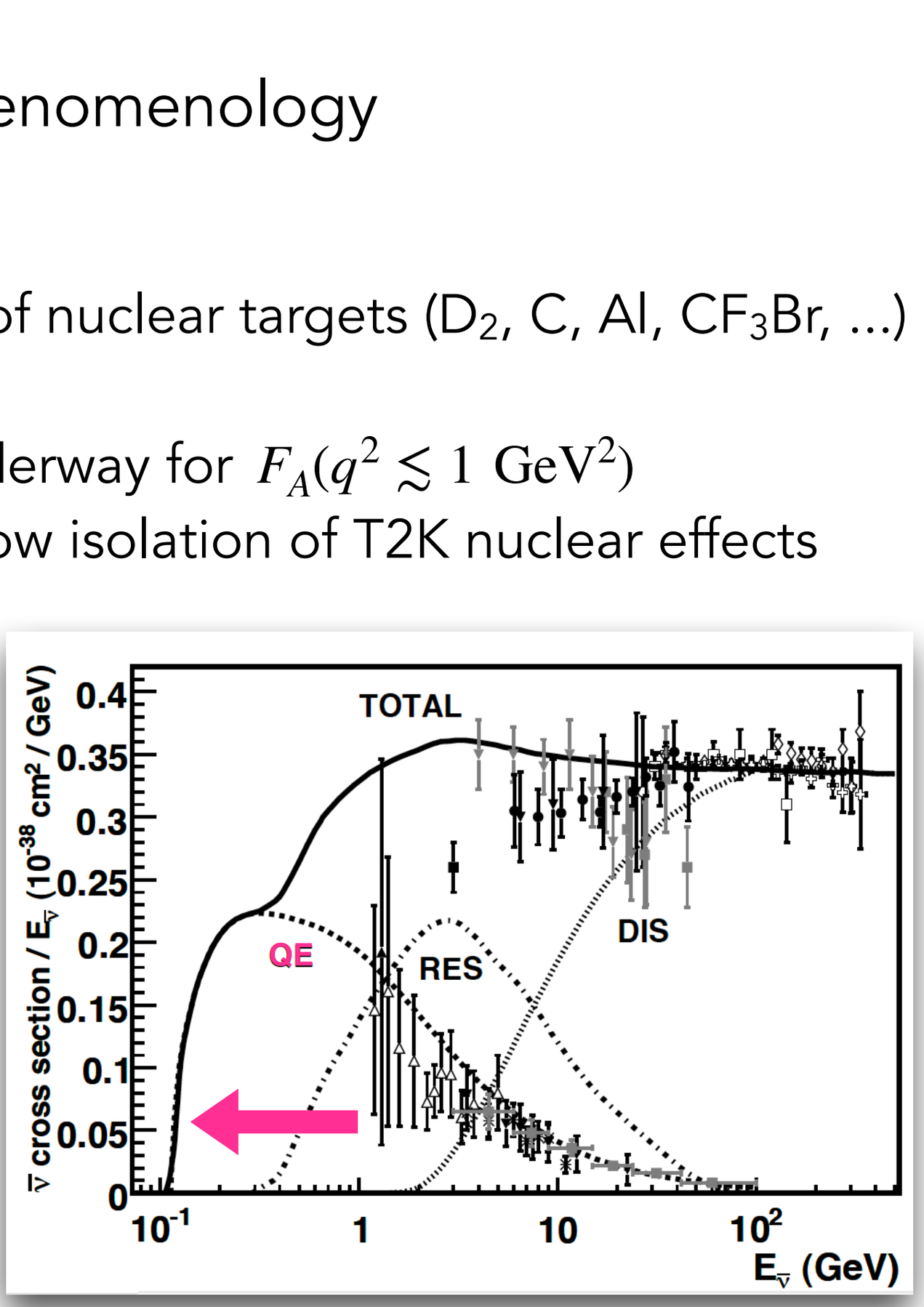

Zeller and Formagio, RMP 84, 1307 (2012)

Experimental precision ~0.2%

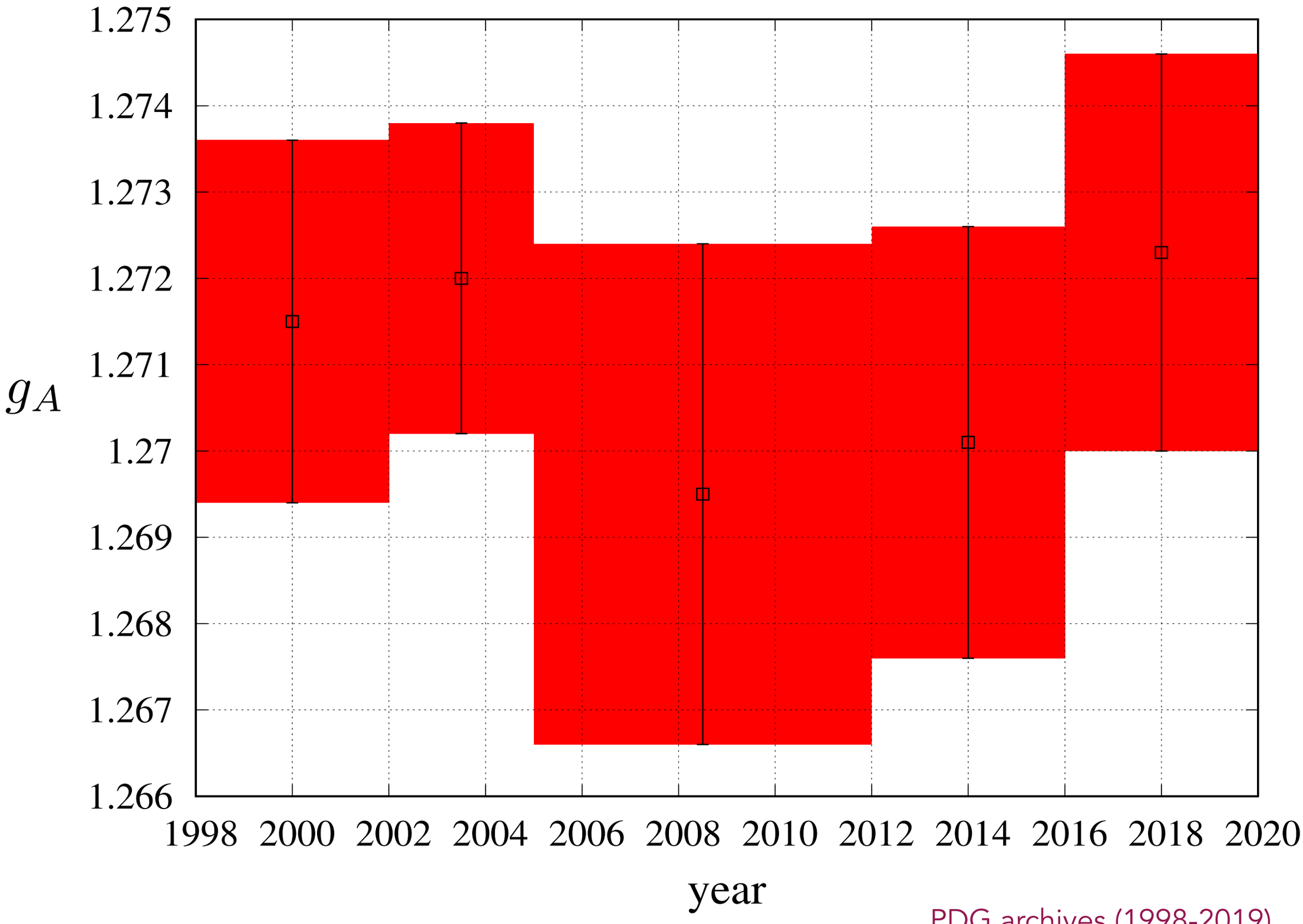

PDG archives (1998-2019)

Slightly more problematic history of calculation...

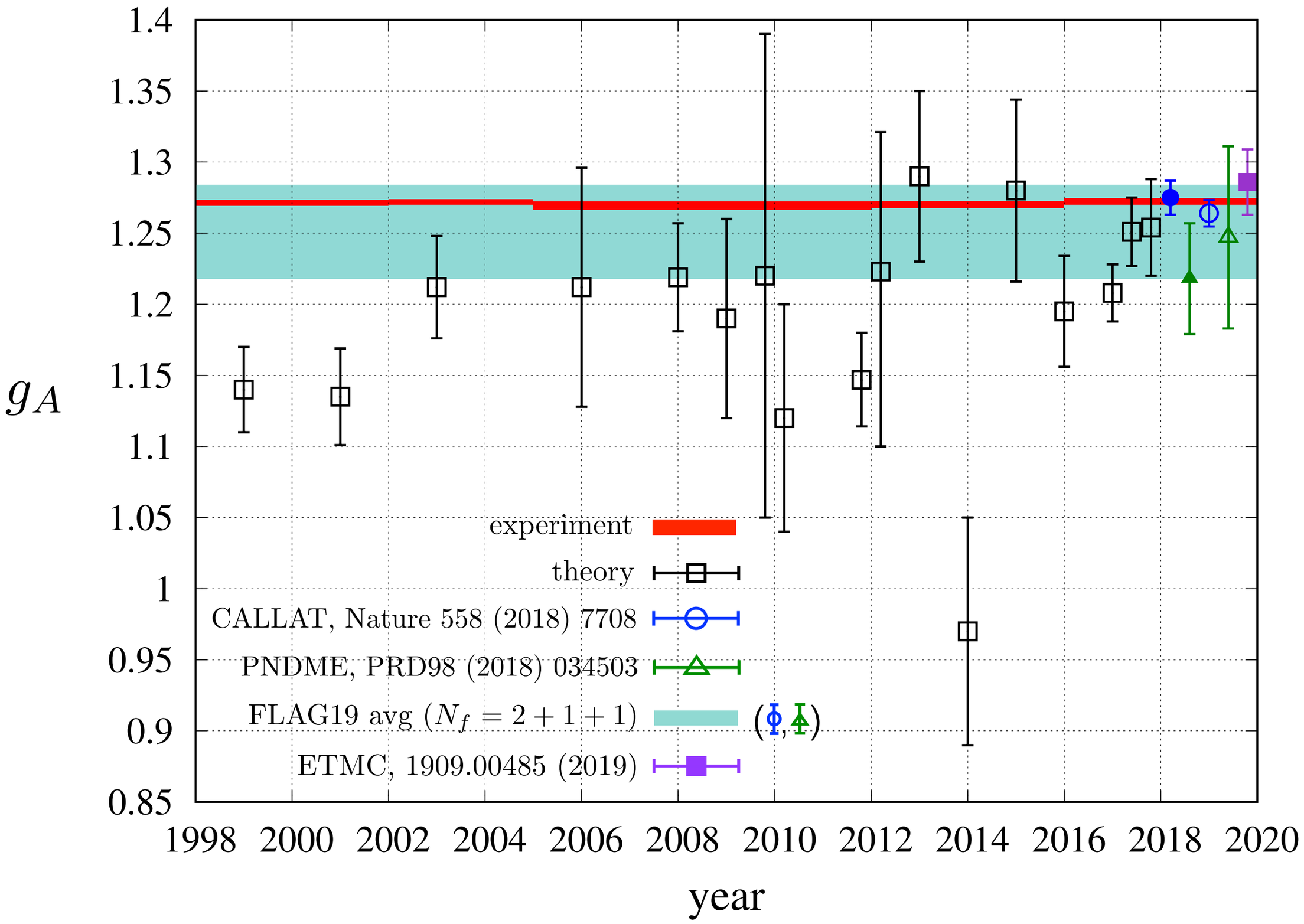

Hard to calculate

- Lattice QCD simulations at $m_q > m_q^{\rm phys}$ and in finite volumes require ChPT... generally difficult for baryons

- baryons notoriously noisy
  - signal $\sim e^{-M_B t}$
  - noise $\sim e^{-\frac{3}{2} M_\pi t}$
  - affects ability to resolve systematic effects, e.g. excited states

- CalLat approach addresses each obstacle

- Introduction
  - g_A and its phenomenology
  - experiment vs theory
- CalLat '18 calculation
  - simulation Berkowitz et al, PRD 96, 054513 (2017)
    - HISQ 2+1+1 gauge fields
    - gradient flow smearing with Möbius DW valence quarks
  - Feynman-Hellmann Theorem inspired approach to correlators
  - renormalization; chiral, continuum, and infinite volume extrapolation
- Summary and outlook

HISQ gauge configuration parameters

abbr.	$N_{\rm cfg}$	volume	$\sim a$ [fm]	m_l/m_s	$\sim m_{\pi_5}$ [MeV]	$\sim m_{\pi_5} L$
a15m400	1000	$16^3 \times 48$	0.15	0.334	400	4.8
a15m350	1000	$16^3 \times 48$	0.15	0.255	350	4.2
a15m310	1960	$16^3 \times 48$	0.15	0.2	310	3.8
a15m220	1000	$24^3 \times 48$	0.15	0.1	220	4.0
a15m130	1000	$32^3 \times 48$	0.15	0.036	130	3.2
a12m400	1000	$24^3 \times 64$	0.12	0.334	400	5.8
a12m350	1000	$24^3 \times 64$	0.12	0.255	350	5.1
a12m310	1053	$24^3 \times 64$	0.12	0.2	310	4.5
a12m220S	1000	$24^3 \times 64$	0.12	0.1	220	3.2
a12m220	1000	$32^3 \times 64$	0.12	0.1	220	4.3
a12m220L	1000	$40^3 \times 64$	0.12	0.1	220	5.4
a12m130	1000	$48^3 \times 64$	0.12	0.036	130	3.9
a09m400	1201	$32^3 \times 64$	0.09	0.335	400	5.8
a09m350	1201	$32^3 \times 64$	0.09	0.255	350	5.1
a09m310	784	$32^3 \times 96$	0.09	0.2	310	4.5
a09m220	1001	$48^3 \times 96$	0.09	0.1	220	4.7

Bazavov et al, PRD 87, 0545 (2013)

MILC HISQ N_f = 2+1+1 gauge fields

- HISQ u,d,s,c sea quarks with discretization effects $\mathcal{O}(\alpha_s a^2, a^4)$
- tadpole improved, 1-loop Symanzik gauge action with $\mathcal{O}(\alpha_s^2 a^2, a^4)$

HISQ gauge configuration parameters

abbr.	N_{cfg}	volume	$\sim a$ [fm]	m_l/m_s	$\sim m_{\pi_5}$ [MeV]	$\sim m_{\pi_5} L$
a15m400	1000	$16^3 \times 48$	0.15	0.334	400	4.8
a15m350	1000	$16^3 \times 48$	0.15	0.255	350	4.2
a15m310	1960	$16^3 \times 48$	0.15	0.2	310	3.8
a15m220	1000	$24^3 \times 48$	0.15	0.1	220	4.0
a15m130	1000	$32^3 \times 48$	0.15	0.036	130	3.2
a12m400	1000	$24^3 \times 64$	0.12	0.334	400	5.8
a12m350	1000	$24^3 \times 64$	0.12	0.255	350	5.1
a12m310	1053	$24^3 \times 64$	0.12	0.2	310	4.5
a12m220S	1000	$24^3 \times 64$	0.12	0.1	220	3.2
a12m220	1000	$32^3 \times 64$	0.12	0.1	220	4.3
a12m220L	1000	$40^3 \times 64$	0.12	0.1	220	5.4
a12m130	1000	$48^3 \times 64$	0.12	0.036	130	3.9
a09m400	1201	$32^3 \times 64$	0.09	0.335	400	5.8
a09m350	1201	$32^3 \times 64$	0.09	0.255	350	5.1
a09m310	784	$32^3 \times 96$	0.09	0.2	310	4.5
a09m220	1001	$48^3 \times 96$	0.09	0.1	220	4.7

MILC HISQ N_f = 2+1+1 gauge fields

- HISQ u,d,s,c sea quarks with discretization effects $\mathcal{O}(\alpha_s a^2, a^4)$
- tadpole improved, 1-loop Symanzik gauge action with $\mathcal{O}(\alpha_s^2 a^2, a^4)$
- to improve extrapolation in m_q, we generated new ensembles

HISQ gauge configuration parameters

abbr.	N_{cfg}	volume	$\sim a$ [fm]	m_l/m_s	$\sim m_{\pi_5}$ [MeV]	$\sim m_{\pi_5} L$
a15m400	1000	$16^3 \times 48$	0.15	0.334	400	4.8
a15m350	1000	$16^3 \times 48$	0.15	0.255	350	4.2
a15m310	1960	$16^3 \times 48$	0.15	0.2	310	3.8
a15m220	1000	$24^3 \times 48$	0.15	0.1	220	4.0
a15m130	1000	$32^3 \times 48$	0.15	0.036	130	3.2
a12m400	1000	$24^3 \times 64$	0.12	0.334	400	5.8
a12m350	1000	$24^3 \times 64$	0.12	0.255	350	5.1
a12m310	1053	$24^3 \times 64$	0.12	0.2	310	4.5
a12m220S	1000	$24^3 \times 64$	0.12	0.1	220	3.2
a12m220	1000	$32^3 \times 64$	0.12	0.1	220	4.3
a12m220L	1000	$40^3 \times 64$	0.12	0.1	220	5.4
a12m130	1000	$48^3 \times 64$	0.12	0.036	130	3.9
a09m400	1201	$32^3 \times 64$	0.09	0.335	400	5.8
a09m350	1201	$32^3 \times 64$	0.09	0.255	350	5.1
a09m310	784	$32^3 \times 96$	0.09	0.2	310	4.5
a09m220	1001	$48^3 \times 96$	0.09	0.1	220	4.7

MILC HISQ N_f = 2+1+1 gauge fields offer

- large statistics

HISQ gauge configuration parameters

abbr.	N_{cfg}	volume	$\sim a$ [fm]	m_l/m_s	$\sim m_{\pi_5}$ [MeV]	$\sim m_{\pi_5} L$
a15m400	1000	$16^3 \times 48$	0.15	0.334	400	4.8
a15m350	1000	$16^3 \times 48$	0.15	0.255	350	4.2
a15m310	1960	$16^3 \times 48$	0.15	0.2	310	3.8
a15m220	1000	$24^3 \times 48$	0.15	0.1	220	4.0
a15m130	1000	$32^3 \times 48$	0.15	0.036	130	3.2
a12m400	1000	$24^3 \times 64$	0.12	0.334	400	5.8
a12m350	1000	$24^3 \times 64$	0.12	0.255	350	5.1
a12m310	1053	$24^3 \times 64$	0.12	0.2	310	4.5
a12m220S	1000	$24^3 \times 64$	0.12	0.1	220	3.2
a12m220	1000	$32^3 \times 64$	0.12	0.1	220	4.3
a12m220L	1000	$40^3 \times 64$	0.12	0.1	220	5.4
a12m130	1000	$48^3 \times 64$	0.12	0.036	130	3.9
a09m400	1201	$32^3 \times 64$	0.09	0.335	400	5.8
a09m350	1201	$32^3 \times 64$	0.09	0.255	350	5.1
a09m310	784	$32^3 \times 96$	0.09	0.2	310	4.5
a09m220	1001	$48^3 \times 96$	0.09	0.1	220	4.7

MILC HISQ N_f = 2+1+1 gauge fields offer

- large statistics
- multiple volumes, including ideal volume study subset

HISQ gauge configuration parameters

abbr.	N_{cfg}	volume	$\sim a$ [fm]	m_l/m_s	$\sim m_{\pi_5}$ [MeV]	$\sim m_{\pi_5} L$
a15m400	1000	$16^3 \times 48$	0.15	0.334	400	4.8
a15m350	1000	$16^3 \times 48$	0.15	0.255	350	4.2
a15m310	1960	$16^3 \times 48$	0.15	0.2	310	3.8
a15m220	1000	$24^3 \times 48$	0.15	0.1	220	4.0
a15m130	1000	$32^3 \times 48$	0.15	0.036	130	3.2
a12m400	1000	$24^3 \times 64$	0.12	0.334	400	5.8
a12m350	1000	$24^3 \times 64$	0.12	0.255	350	5.1
a12m310	1053	$24^3 \times 64$	0.12	0.2	310	4.5
a12m220S	1000	$24^3 \times 64$	0.12	0.1	220	3.2
a12m220	1000	$32^3 \times 64$	0.12	0.1	220	4.3
a12m220L	1000	$40^3 \times 64$	0.12	0.1	220	5.4
a12m130	1000	$48^3 \times 64$	0.12	0.036	130	3.9
a09m400	1201	$32^3 \times 64$	0.09	0.335	400	5.8
a09m350	1201	$32^3 \times 64$	0.09	0.255	350	5.1
a09m310	784	$32^3 \times 96$	0.09	0.2	310	4.5
a09m220	1001	$48^3 \times 96$	0.09	0.1	220	4.7

MILC HISQ N_f = 2+1+1 gauge fields offer

- large statistics
- multiple volumes, including ideal volume study subset
- range of lattice spacings

HISQ gauge configuration parameters

abbr.	N_{cfg}	volume	$\sim a$ [fm]	m_l/m_s	$\sim m_{\pi_5}$ [MeV]	$\sim m_{\pi_5} L$
a15m400	1000	$16^3 \times 48$	0.15	0.334	400	4.8
a15m350	1000	$16^3 \times 48$	0.15	0.255	350	4.2
a15m310	1960	$16^3 \times 48$	0.15	0.2	310	3.8
a15m220	1000	$24^3 \times 48$	0.15	0.1	220	4.0
a15m130	1000	$32^3 \times 48$	0.15	0.036	130	3.2
a12m400	1000	$24^3 \times 64$	0.12	0.334	400	5.8
a12m350	1000	$24^3 \times 64$	0.12	0.255	350	5.1
a12m310	1053	$24^3 \times 64$	0.12	0.2	310	4.5
a12m220S	1000	$24^3 \times 64$	0.12	0.1	220	3.2
a12m220	1000	$32^3 \times 64$	0.12	0.1	220	4.3
a12m220L	1000	$40^3 \times 64$	0.12	0.1	220	5.4
a12m130	1000	$48^3 \times 64$	0.12	0.036	130	3.9
a09m400	1201	$32^3 \times 64$	0.09	0.335	400	5.8
a09m350	1201	$32^3 \times 64$	0.09	0.255	350	5.1
a09m310	784	$32^3 \times 96$	0.09	0.2	310	4.5
a09m220	1001	$48^3 \times 96$	0.09	0.1	220	4.7

MILC HISQ N_f = 2+1+1 gauge fields offer

- large statistics
- multiple volumes, including ideal volume study subset
- range of lattice spacings
- range of quark masses, including physical values

Gradient flow smearing

Narayanan and Neuberger, JHEP 03, 064 (2006)
Luscher and Weisz, JHEP 02, 051 (2011)
Luscher, JHEP 04, 123 (2013)

- begin with 4d gauge fields $A_\mu(x)$
- extend to continuous 5th dimension, t, via $B_\mu(t,x)$ for all μ s.t.

$$B_\mu(0,x) = A_\mu(x)$$

- diffusion equation drives "flow" in t toward classical minimum

$$\partial_t B_\mu = D_\nu G_{\nu\mu}$$

- common for scale setting, e.g., for $E = \frac{1}{4} B^a_{\mu\nu} B^a_{\mu\nu}$

$$\left(t\,\partial_t [t^2 E(t)]\right)\Big|_{t=w_0^2} = 0.3$$

- introduces length scale $l_{gf} \sim a\sqrt{8t}$ that smears out UV physics
- t will be t_{gf} throughout rest of talk

Gradient flow smearing with Möbius Domain Wall

M_N/F_π ($M_\pi \approx 310$ MeV)

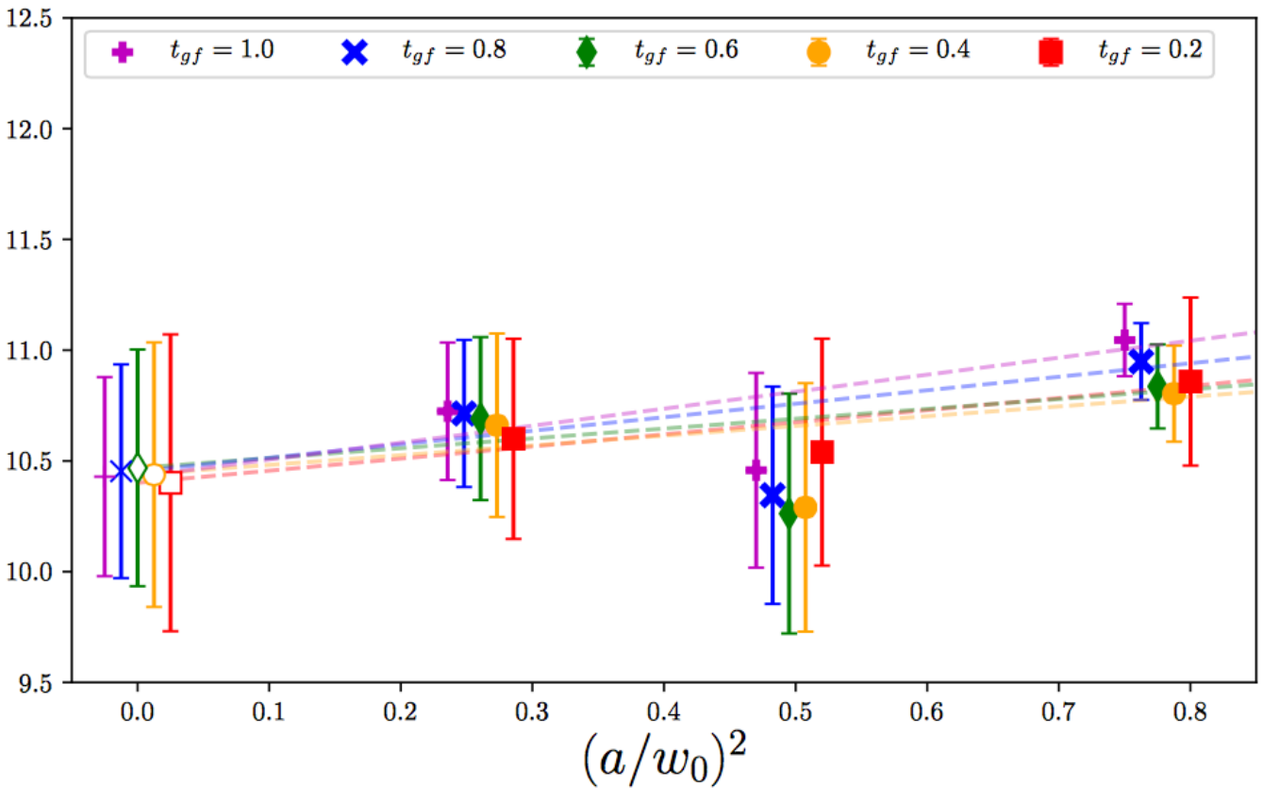

Z_A ($M_\pi \approx 310$ MeV)

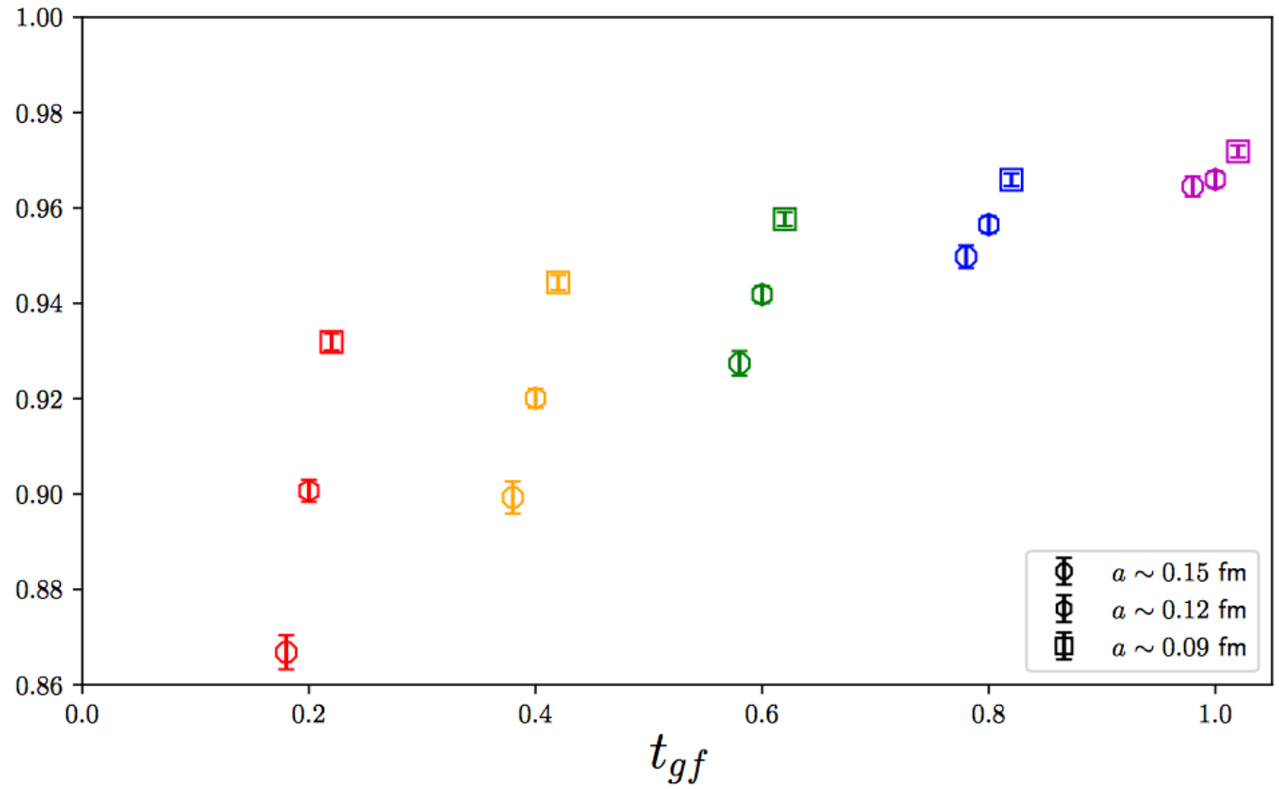

we find:

- reduced discretization effects, e.g. $Z_A = Z_V + \mathcal{O}(a^2) \sim 1$
- continuum extrapolation independent of flow
- improved stochastic uncertainties

- Introduction
  - g_A and its phenomenology
  - experiment vs theory
- CalLat '18 calculation
  - simulation
    - HISQ 2+1+1 gauge fields
    - gradient flow smearing with Möbius DW valence quarks
  - Feynman-Hellmann Theorem inspired approach to correlators

    Bouchard et al, PRD 96, 014504 (2017)
  - renormalization; chiral, continuum, and infinite volume extrapolation
- Summary and outlook

Standard approach to 3pt correlators

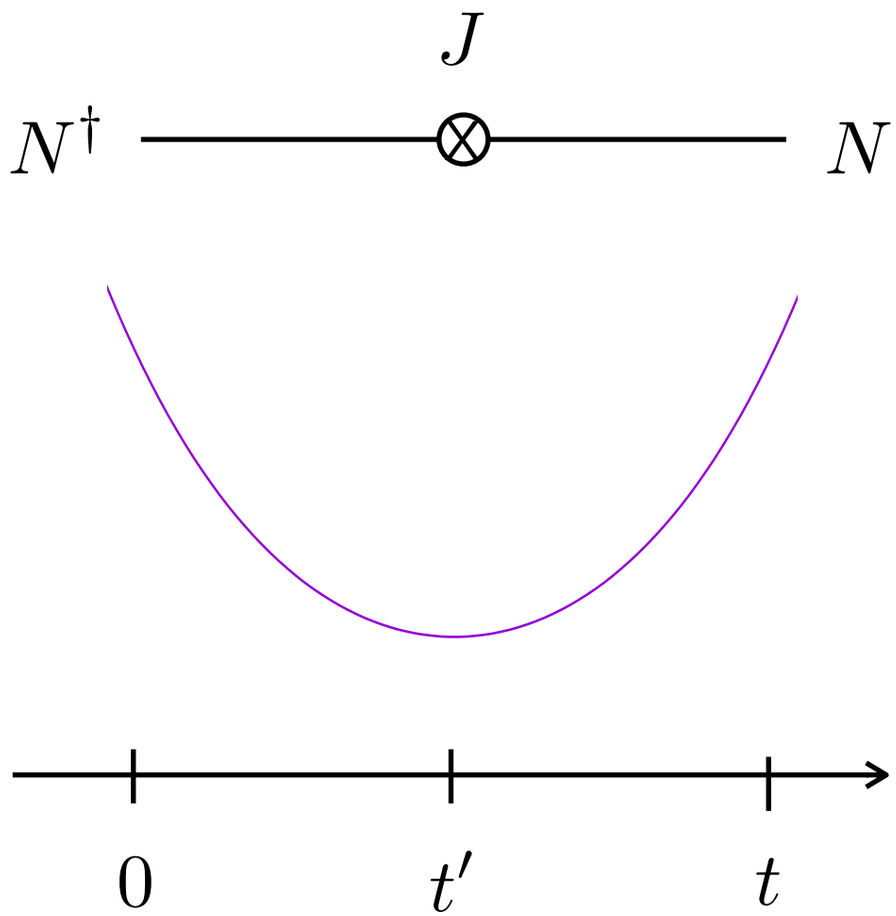

- generate data for (a handful of) fixed t
- extract matrix elements from t and t' dependence
- signal (and signal to noise) decays from both ends
- need plateau and/or control over excited states

... an example. PNDME, PRD98 (2018) 034503

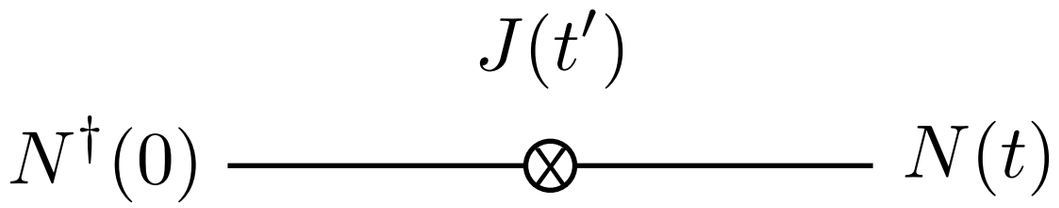

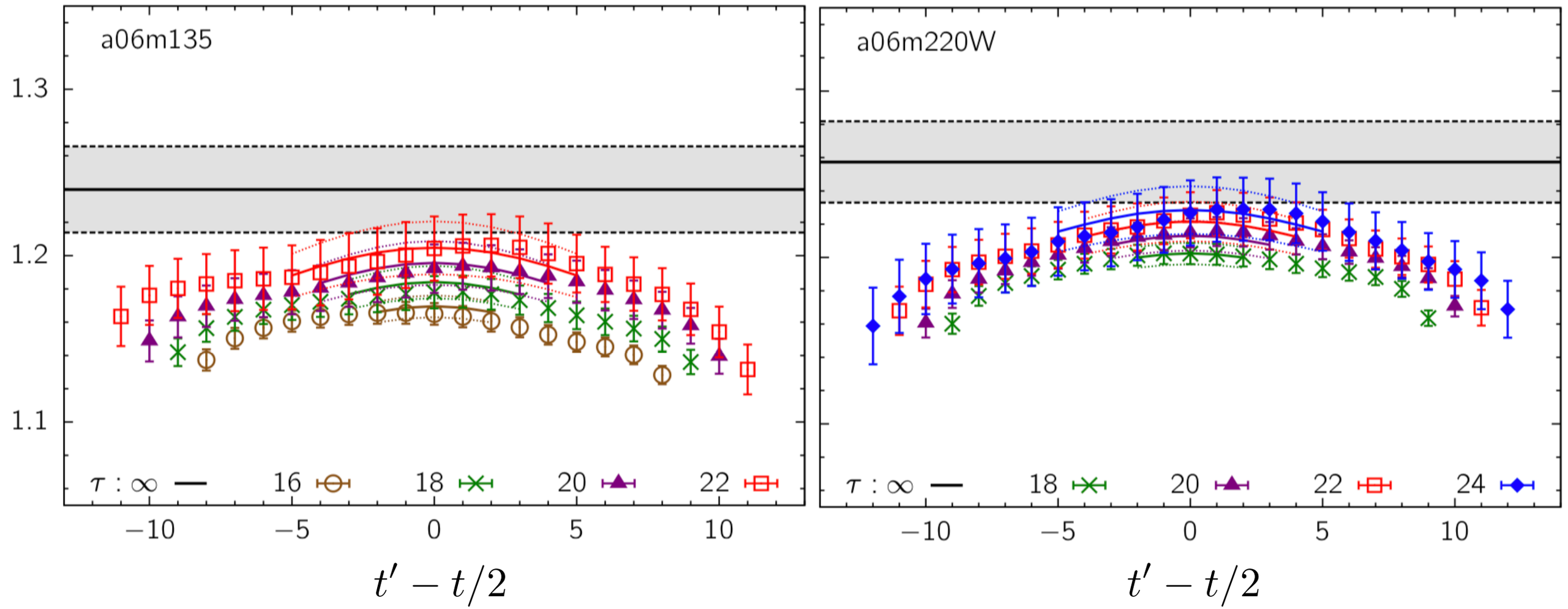

- must fit dependence on both t' and t
- for plot on right, 84 data points ⇒ data covariance matrix is big
- to control it, omitted the 7 t' nearest the source/sink

Simpler for 2pt correlators

$$N^\dagger(0) \longrightarrow N(t)$$

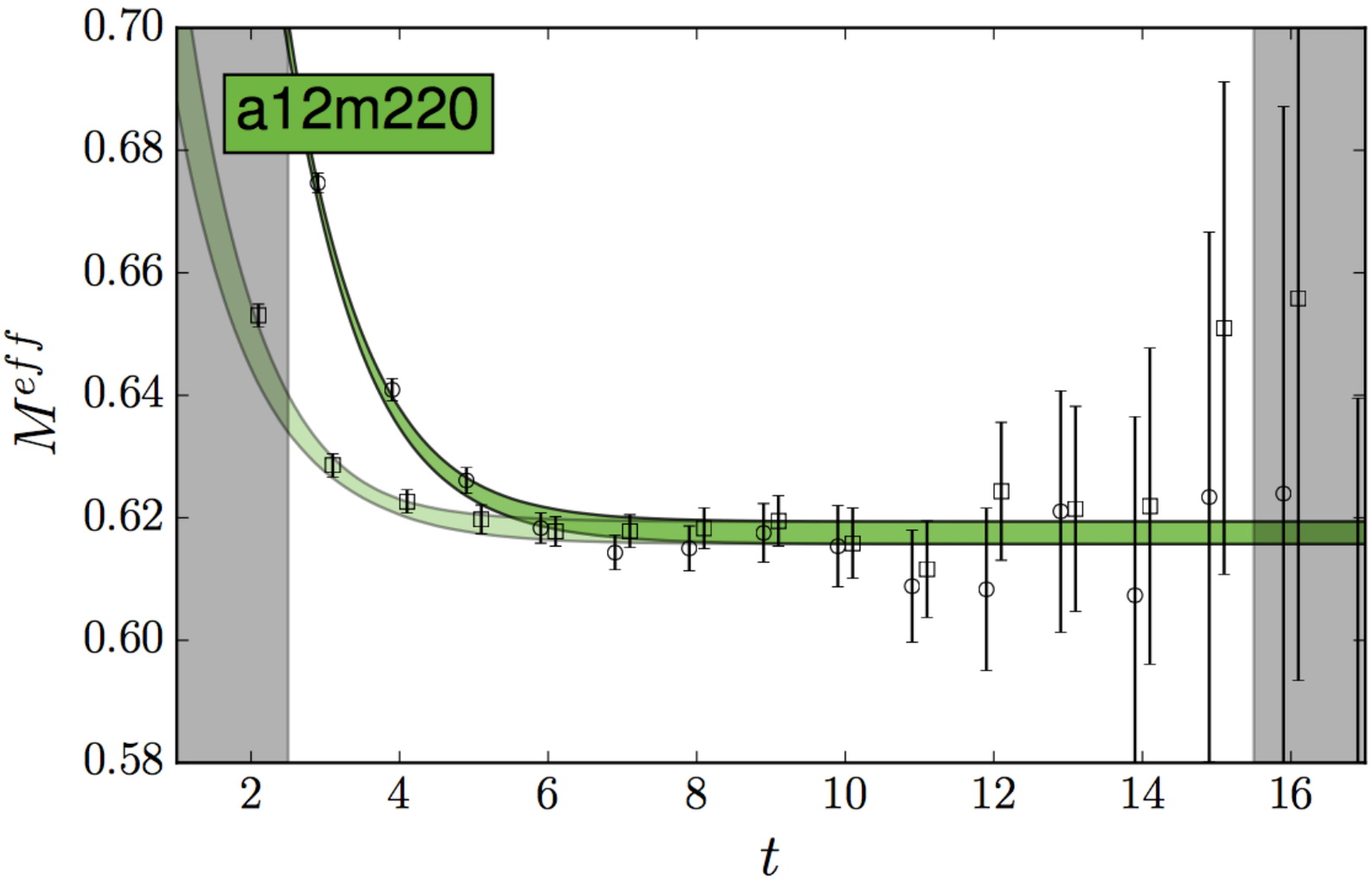

- asymptotes to ground state at large t
- want 2 pt-like time dependence from 3 pt correlators...

Feynman-Hellmann Theorem

- For a Hamiltonian with a linear interaction term $\lambda\hat{H}_\lambda$

$$\hat{H} = \hat{H}_0 + \lambda\hat{H}_\lambda,$$

- energy eigenstates $|\psi_\lambda\rangle$ and eigenvalues E_λ

$$\hat{H}|\psi_\lambda\rangle = E_\lambda|\psi_\lambda\rangle,$$

- the matrix element of the interaction is related to the variation of the spectrum,

$$\frac{\partial E_\lambda}{\partial\lambda} = \langle\psi_\lambda|\hat{H}_\lambda|\psi_\lambda\rangle.$$

Güttinger, Z Phys 73, 169–184 (1932)
Pauli, Handbuch der Physik, v24, 162 (1933)
Hellmann, Z Phys 85,180–190 (1933)
Hellmann, (1937)
Feynman, Phys Rev 56, 340–343 (1939)

Feynman-Hellmann Theorem inspired

- Add linear interaction to the action

$$S \to S_\lambda = S + \lambda \int dt'\, J(t')$$

- modifying the vacuum and partition function

$$|\Omega\rangle \to |\Omega_\lambda\rangle, \quad Z \to Z_\lambda = \int D\Phi\; e^{-S_\lambda}$$

- and the 2 pt correlation function

$$C_\lambda(t) = \langle \Omega_\lambda | T\{N(t)N^\dagger(0)\} | \Omega_\lambda \rangle$$

$$= \frac{1}{Z_\lambda} \int D\Phi\; T\{N(t)N^\dagger(0)\}\; e^{-S_\lambda}$$

Feynman-Hellmann Theorem inspired

- The derivative with respect to the interaction coupling

$$\left.\frac{\partial C_\lambda(t)}{\partial\lambda}\right|_{\lambda=0} = C(t)\int dt' \langle\Omega|J(t')|\Omega\rangle - \int dt' \langle\Omega| T\left\{N(t)J(t')N^\dagger(0)\right\}|\Omega\rangle$$

- (and Feynman-Hellmann Theorem) suggest derivative of

$$M_\lambda^{eff}(t) = \ln\left(\frac{C_\lambda(t)}{C_\lambda(t+1)}\right)$$

$$\Rightarrow \left.\frac{\partial M_\lambda^{eff}(t)}{\partial\lambda}\right|_{\lambda=0} = \left[\frac{\partial_\lambda C_\lambda(t)}{C(t)} - \frac{\partial_\lambda C_\lambda(t+1)}{C(t+1)}\right]_{\lambda=0}$$

Feynman-Hellmann Theorem inspired

- behavior of $\partial_\lambda M_\lambda^{eff}(t)\big|_{\lambda=0}$ with t

$$\left.\frac{\partial M_\lambda^{eff}(t)}{\partial\lambda}\right|_{\lambda=0} = \left[\frac{\partial_\lambda C_\lambda(t)}{C(t)} - \frac{\partial_\lambda C_\lambda(t+1)}{C(t+1)}\right]_{\lambda=0}$$

- spectral decomposition of $\partial_\lambda C_\lambda(t)\big|_{\lambda=0}$

$$-\left.\frac{\partial C_\lambda(t)}{\partial\lambda}\right|_{\lambda=0} = \sum_{n=0}^{N-1}[(t-1)|z_n|^2 g_{nn} + d_n]e^{-E_n t} + \sum_{\substack{n,m=0\\ n\neq m}}^{N-1} z_n g_{nm} z_m^\dagger \frac{e^{-E_n t}e^{\frac{\Delta_{nm}}{2}} - e^{-E_m t}e^{\frac{\Delta_{mn}}{2}}}{e^{\frac{\Delta_{mn}}{2}} - e^{\frac{\Delta_{nm}}{2}}}$$

- in the long-t limit

$$\lim_{t\to\infty}\partial_\lambda M_\lambda^{eff}(t)\big|_{\lambda=0} = g_{00} \qquad \left(\text{note:}\quad g_{00} = \frac{g_A}{2M_N}\right)$$

That 3 pt matrix elements can be obtained by varying a 2 pt correlator is not new... used extensively in LQCD

Chambers et al, PRD 90, 014510 (2014)

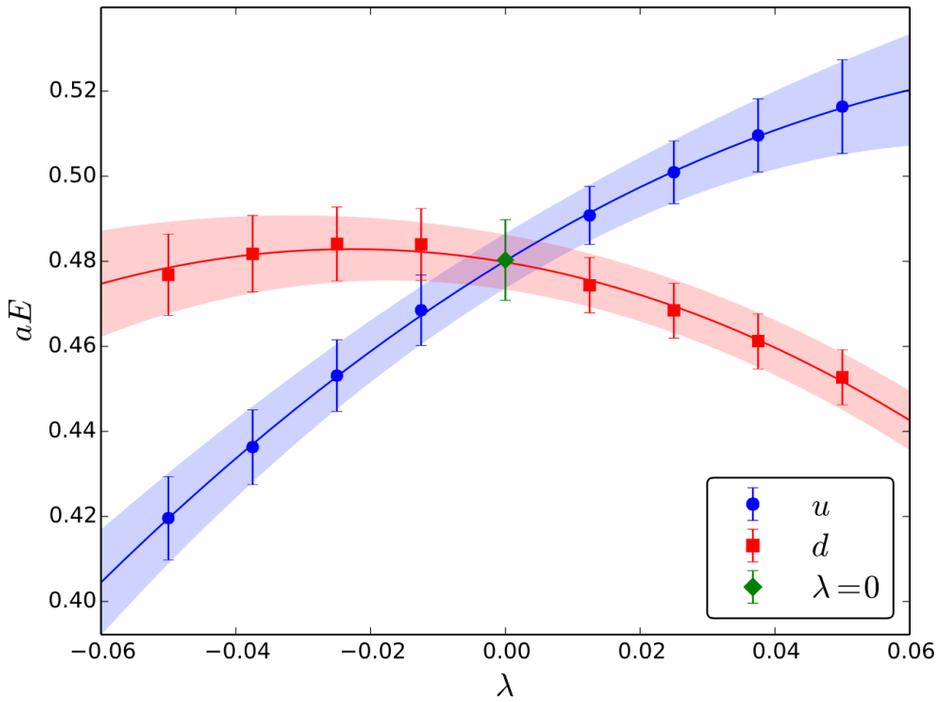

Savage et al, PRL 119, 062002 (2017)

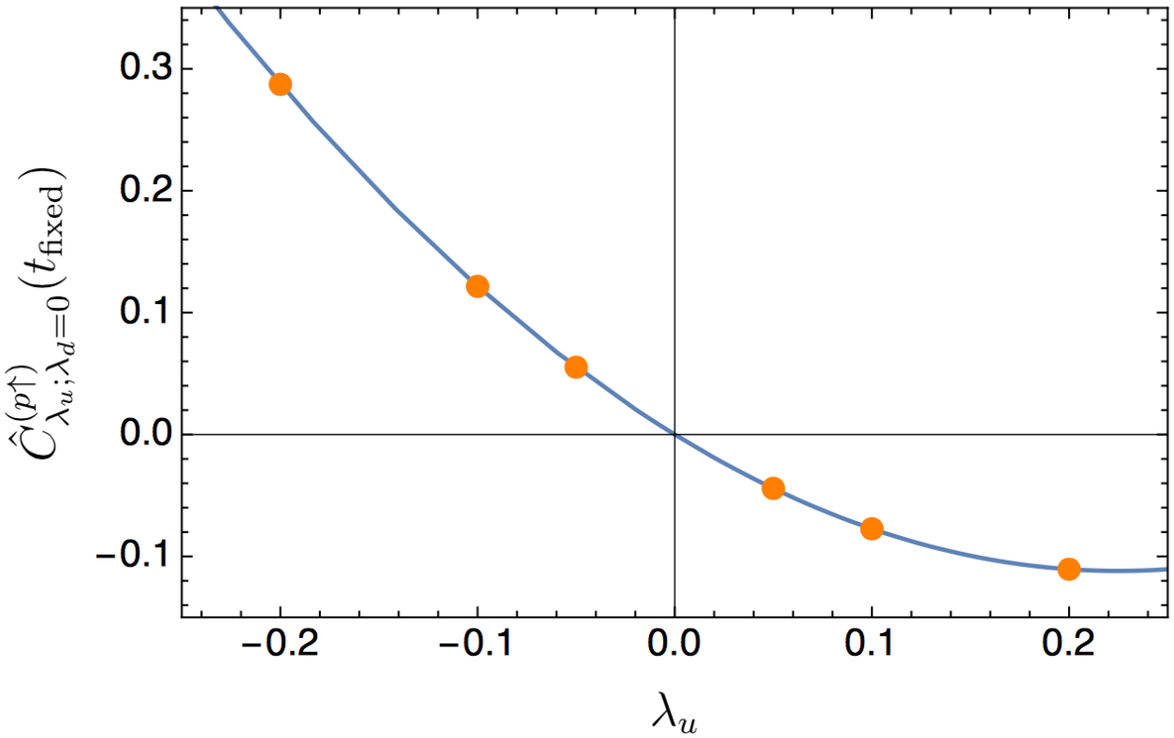

Chambers et al find $\partial_\lambda E_\lambda\big|_{\lambda=0}$ to extract proton g_A and connected quark contributions to baryon spin.

Savage et al find $\partial_\lambda C_\lambda(t)\big|_{\lambda=0}$ to extract proton g_A and matrix elements for pp fusion and tritium beta decay.

... can be traced back to
- Martinelli, Parisi, Petronzio, and Rapuano PLB 116, 434 (1982)
- Fucito, Parisi, and Petrarca, PLB 115, 148 (1982)
- Bernard, Draper, Olynyk, and Rushton, PRL 49, 1076 (1982)

The difference

- build $\partial_\lambda C_\lambda(t)\big|_{\lambda=0}$ analytically - no need to evaluate at multiple λ

$$\left.\frac{\partial C_\lambda(t)}{\partial\lambda}\right|_{\lambda=0} = C(t)\int dt' \langle\Omega|J(t')|\Omega\rangle - \int dt' \langle\Omega| T\left\{N(t)J(t')N^\dagger(0)\right\}|\Omega\rangle$$

- sum over current insertions during propagator construction

Maiani et al, NPB 293, 420 (1987)

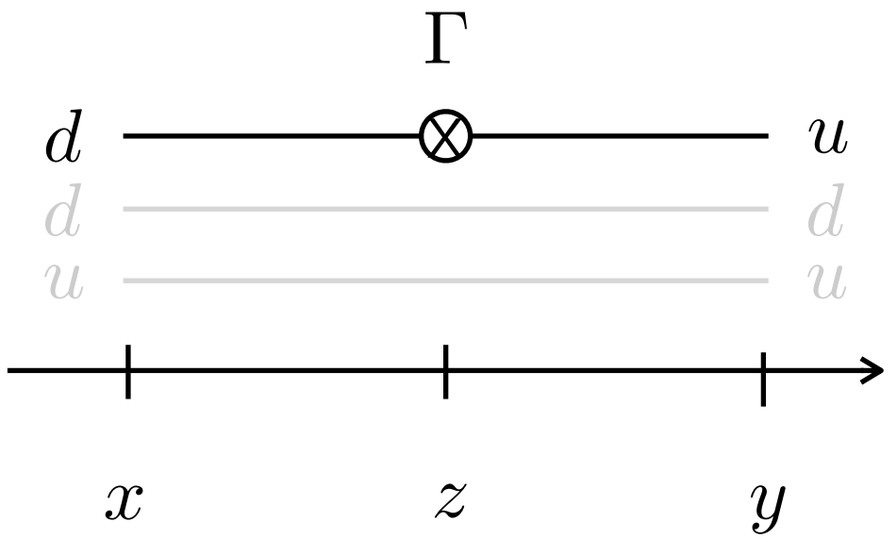

$$S^\Gamma(y,x) = \sum_{z=(t_z,\vec{z})} S(y,z)\Gamma S(z,x)$$

- generates **data for all source-sink separations**, $t = t_y - t_x$

correlator fit results

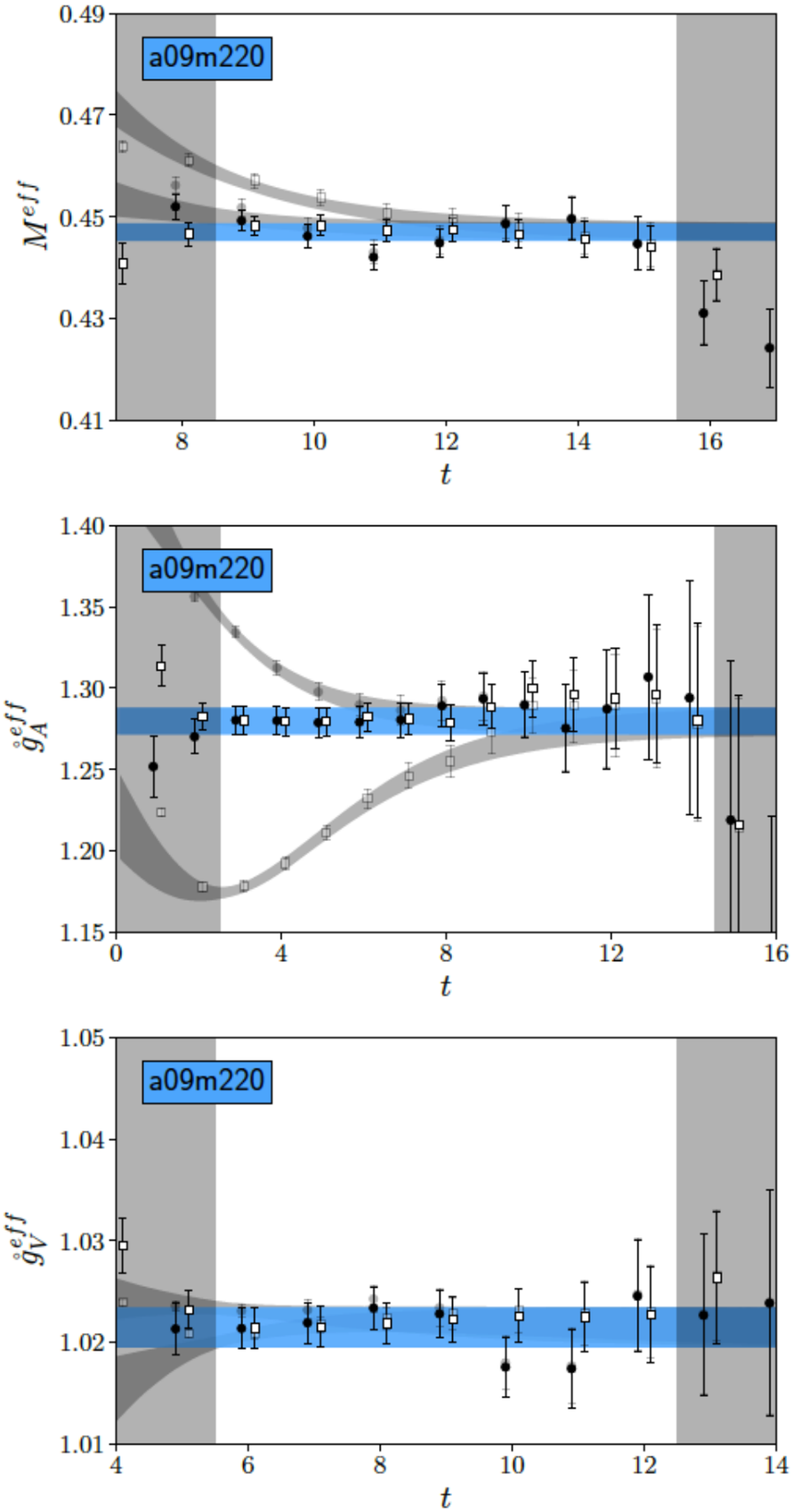

- simultaneous fit to

$$M^{eff}(t),\ \mathring{g}_A^{eff},\ \mathring{g}_V^{eff}$$

- raw data in gray along with fit results
- black/white filled results subtract excited state fitted contributions from raw data
- construct correlated ratio

$$\mathring{g}_A^{eff} / \mathring{g}_V^{eff}$$

- **more data** than standard method

$\Rightarrow$ resolve excited states and leverage precise data at small t

- Introduction
  - g_A and its phenomenology
  - experiment vs theory
- CalLat '18 calculation
  - simulation
    - HISQ 2+1+1 gauge fields
    - gradient flow smearing with Möbius DW valence quarks
  - Feynman-Hellmann Theorem inspired approach to correlators
  - renormalization; chiral, continuum, and infinite volume extrapolation
- Summary and outlook

Renormalization

- from analyzing FHT correlators $\mathring{g}_A / \mathring{g}_V$
- calculate matching factors Z_A / Z_V using nonperturbative Rome-Southampton method

Martinelli et al, NPB 445, 81 (1995)
Aoki et al, PRD 78, 054510 (2008)
Sturm et al, PRD 80, 014501 (2009)

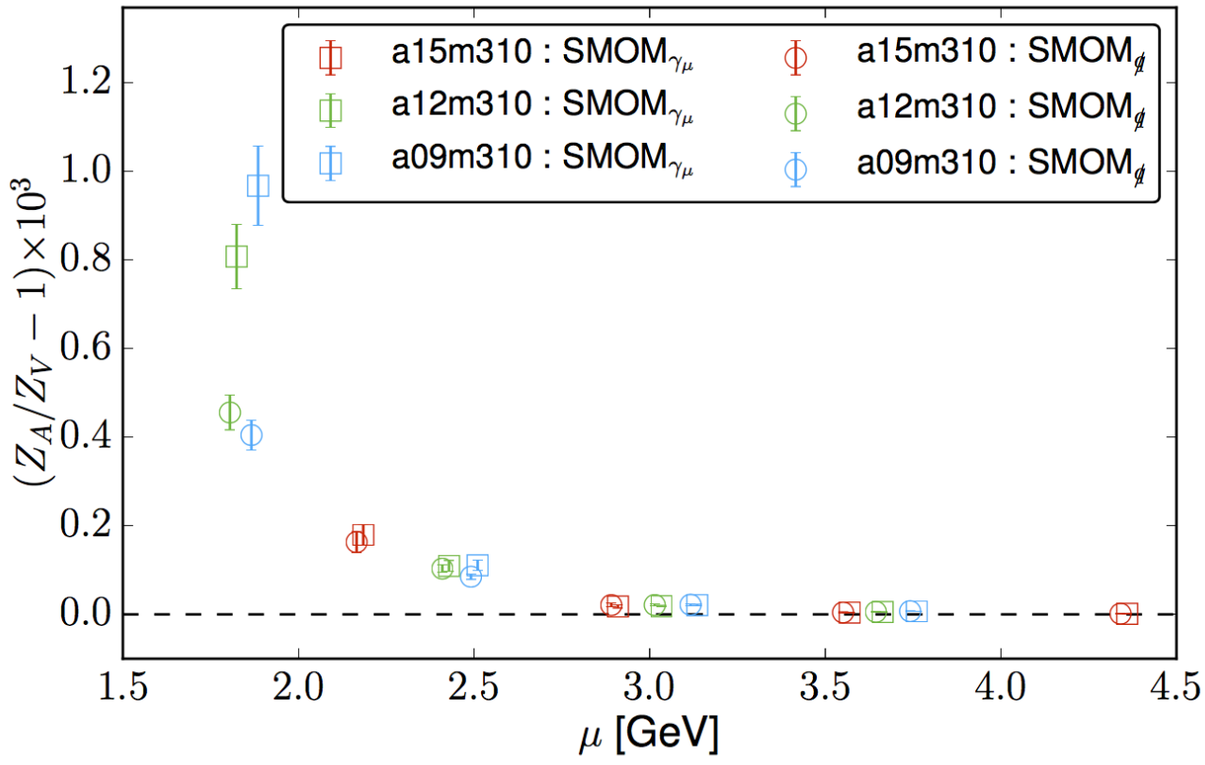

- conserved vector current ensures $Z_V \mathring{g}_V = 1$, therefore

$$g_A = \frac{Z_A}{Z_V} \frac{\mathring{g}_A}{\mathring{g}_V}$$

Chiral, continuum, and infinite volume extrapolation

- dimensionless quantities parameterize dependence

$$\epsilon_\pi = \frac{m_\pi}{4\pi F_\pi},\ \epsilon_a^2 = \frac{a^2}{4\pi w_0^2},\ m_\pi L$$

- chiral extrapolation options:

Jenkins and Manohar, PLB 259, 353 (1991)
V. Bernard et al, NPB 388, 315 (1992)
Kambor and Mojzis, JHEP 04, 031 (1999)

  - SU(2) HBχPT

(1) $$g_A^{\chi\mathrm{PT}} = g_0 + c_2\epsilon_\pi^2 - \epsilon_\pi^2(g_0 + 2g_0^3)\ln(\epsilon_\pi^2) + g_0 c_3 \epsilon_\pi^3 + c_4\epsilon_\pi^4$$

LO NLO NNLO NNNLO ct

  - Taylor series expansions

(2) $$g_A^{\mathrm{Taylor},\ \epsilon_\pi^2} = c_0 + c_2\epsilon_\pi^2 + c_4\epsilon_\pi^4$$

LO NLO NNLO

(3) $$g_A^{\mathrm{Taylor},\ \epsilon_\pi} = c_0 + c_1\epsilon_\pi + c_2\epsilon_\pi^2$$

LO NLO NNLO

Chiral, continuum, and infinite volume extrapolation

- continuum extrapolation Chen et al, PRD 79, 117502 (2009)

$$\delta_a = a_2\epsilon_a^2 + b_4\epsilon_a^2\epsilon_\pi^2 + a_4\epsilon_a^4$$

- infinite volume extrapolation
  - include FV corrections through NLO Beane and Savage, PRD 70, 074029 (2004)

$$\delta_L = \frac{8}{3}\epsilon_\pi^2[g_0^3 F_1(m_\pi L) + g_0 F_3(m_\pi L)]$$

  - accommodate higher order with unknown coefficient f_3

$$\delta_{L_3} = f_3\epsilon_\pi^3 F_1(m_\pi L)$$

  - total finite volume correction

$$\delta'_L = \delta_L + \delta_{L_3}$$

Chiral, continuum, and infinite volume extrapolation

- 6 models based on 3 chiral extrapolation options

$$\text{NNLO } \chi\text{PT}: \;\; g_0 + c_2\epsilon_\pi^2 - \epsilon_\pi^2(g0 + 2g_0^3)\ln(\epsilon_\pi^2) + g_0 c_3 \epsilon_\pi^3 + \delta_a + \delta'_L$$

$$\text{NNLO+ct } \chi\text{PT}: \;\; g_0 + c_2\epsilon_\pi^2 - \epsilon_\pi^2(g0 + 2g_0^3)\ln(\epsilon_\pi^2) + g_0 c_3 \epsilon_\pi^3 + c_4\epsilon_\pi^4 + \delta_a + \delta'_L$$

$$\text{NLO Taylor } \epsilon_\pi^2: \;\; c_0 + c_2\epsilon_\pi^2 + \delta_a + \delta'_L$$

$$\text{NNLO Taylor } \epsilon_\pi^2: \;\; c_0 + c_2\epsilon_\pi^2 + c_4\epsilon_\pi^4 + \delta_a + \delta'_L$$

$$\text{NLO Taylor } \epsilon_\pi: \;\; c_0 + c_1\epsilon_\pi + \delta_a + \delta'_L$$

$$\text{NNLO Taylor } \epsilon_\pi: \;\; c_0 + c_1\epsilon_\pi + c_2\epsilon_\pi^2 + \delta_a + \delta'_L$$

- apriori, all models on equal footing
  - weighted, correlated average over models includes model uncertainty

Fit each model

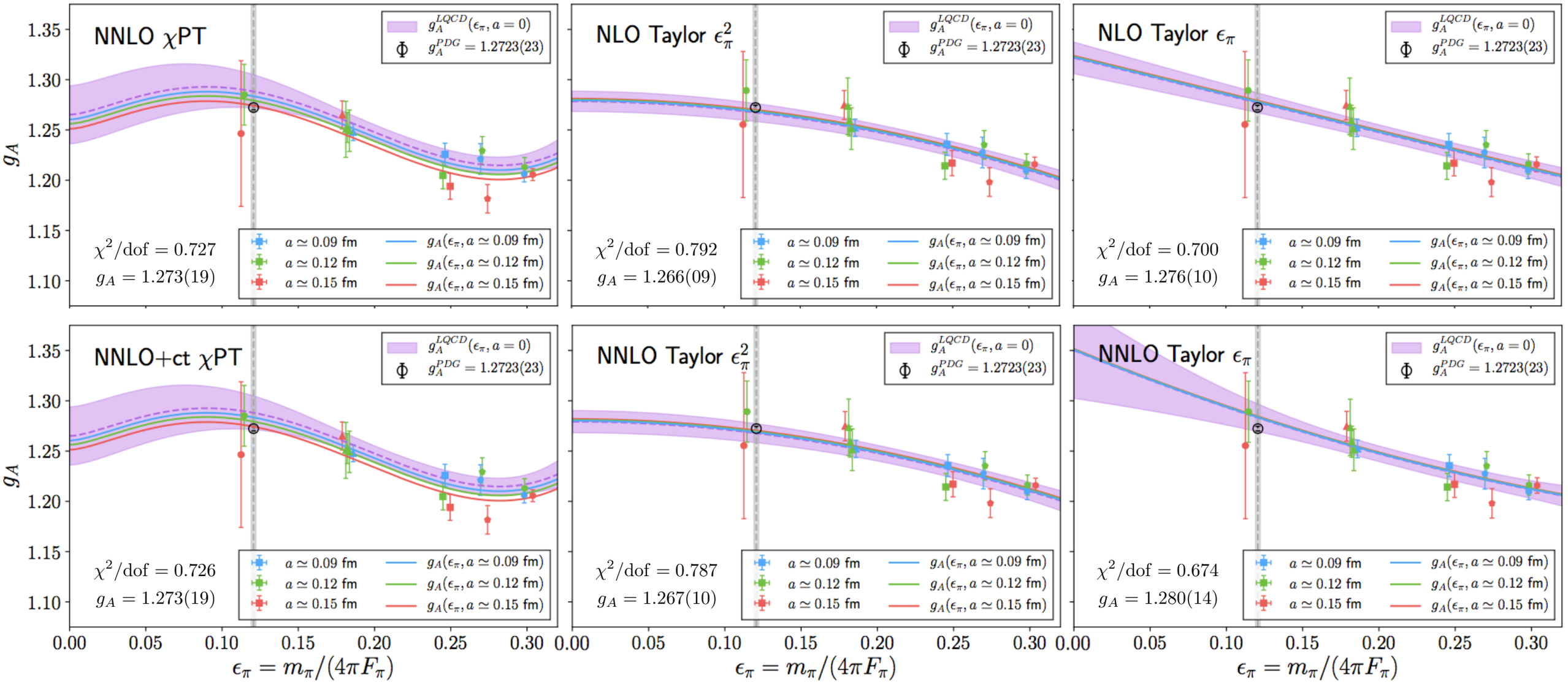

- each fit has acceptable χ^2/dof
- all model fits are consistent
- we average over models, weighted by relative probability

Averaging over models

Given data D and models M_k , average model results $g_A(M_k)$, each with probability $P(M_k|D)$ from Bayes' Theorem,

$$P(M_k|D) = \frac{P(D|M_k)P(M_k)}{\sum_n P(D|M_n)P(M_n)}.$$

The resulting model average is

$$g_A(\text{model average}) = \sum_k g_A(M_k)P(M_k|D).$$

M_k (model)	χ^2/dof	$P(M_k\|D)$	$g_A(M_k)$
NNLO χPT	0.727	0.033	1.273(19)
NNLO+ct χPT	0.726	0.033	1.273(19)
NLO Taylor ϵ_π^2	0.792	0.287	1.266(09)
NNLO Taylor ϵ_π^2	0.787	0.284	1.267(10)
NLO Taylor ϵ_π	0.700	0.191	1.276(10)
NNLO Taylor ϵ_π	0.674	0.172	1.280(14)
model average			1.271(11)(06)

Averaging over models

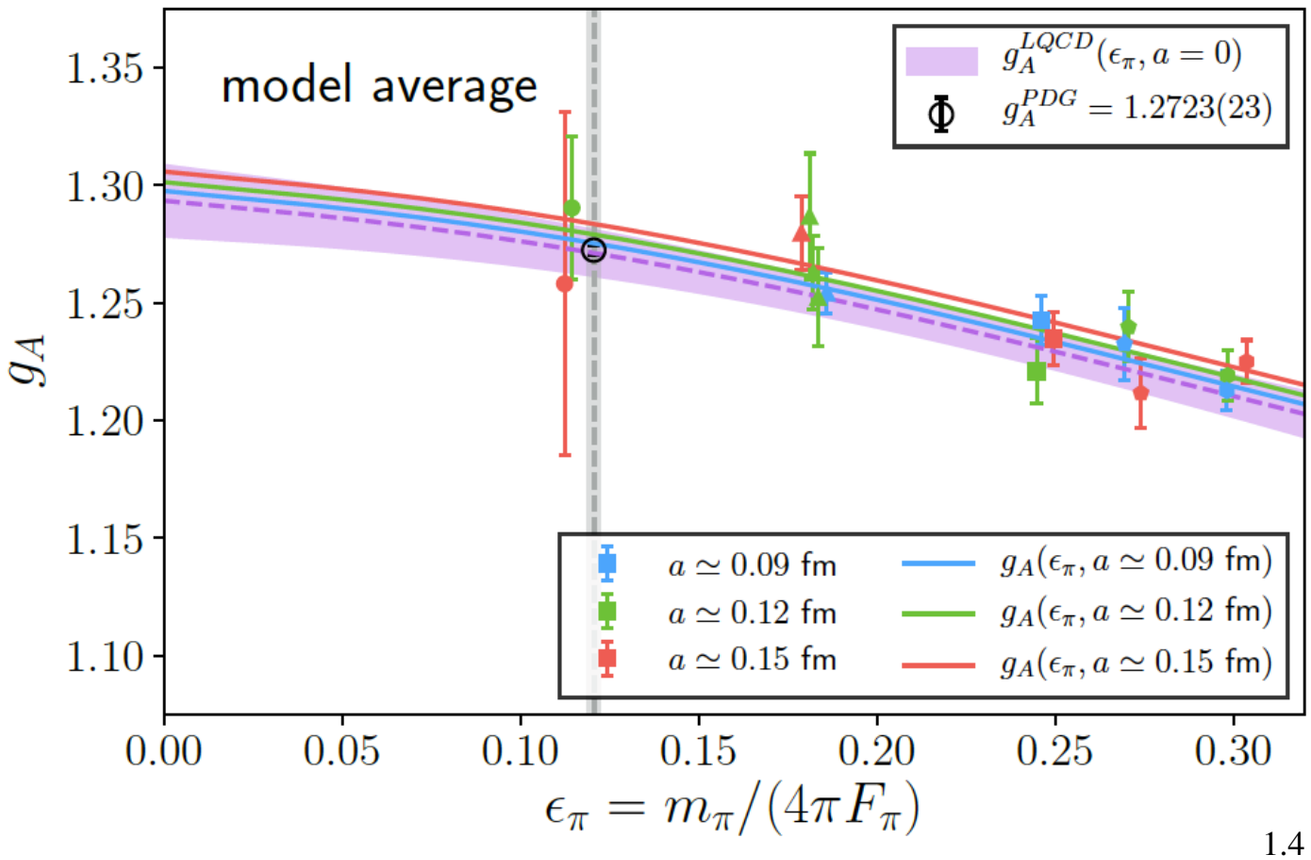

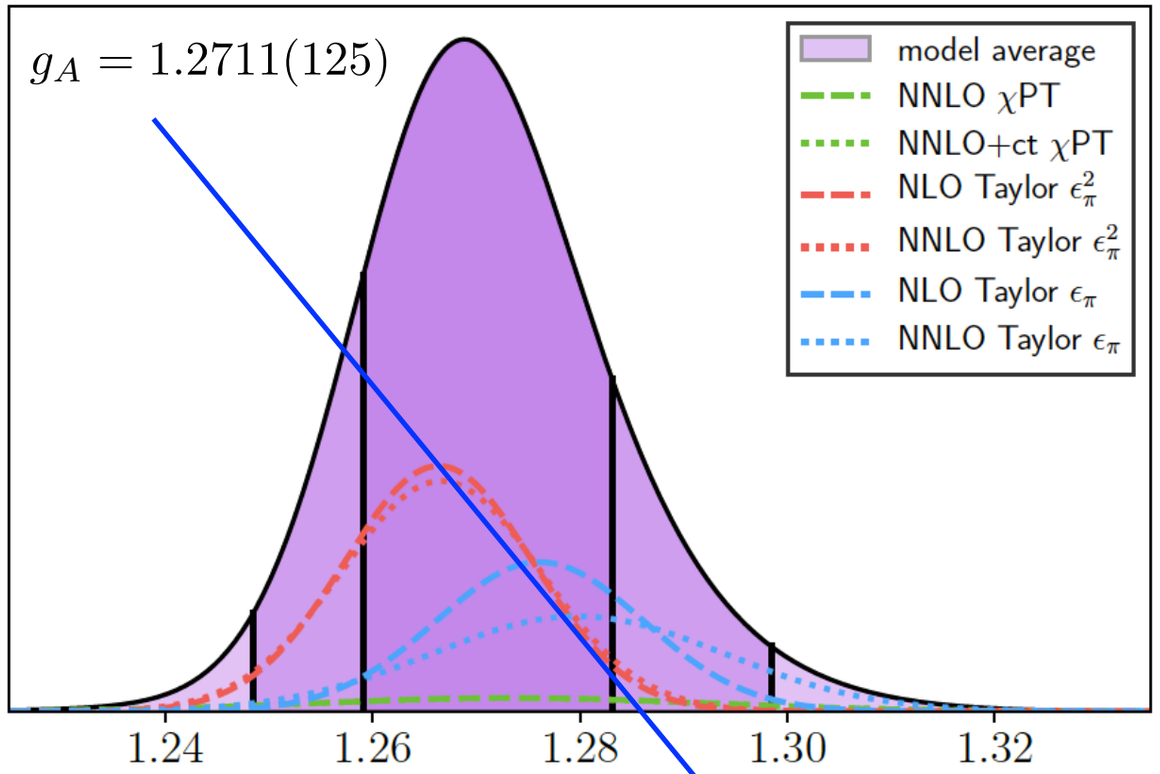

Error Budget	%
statistical	0.81
chiral extrapolation	0.31
continuum extrapolation	0.12
infinite volume	0.15
isospin breaking	0.03
model selection	0.43
total	0.99

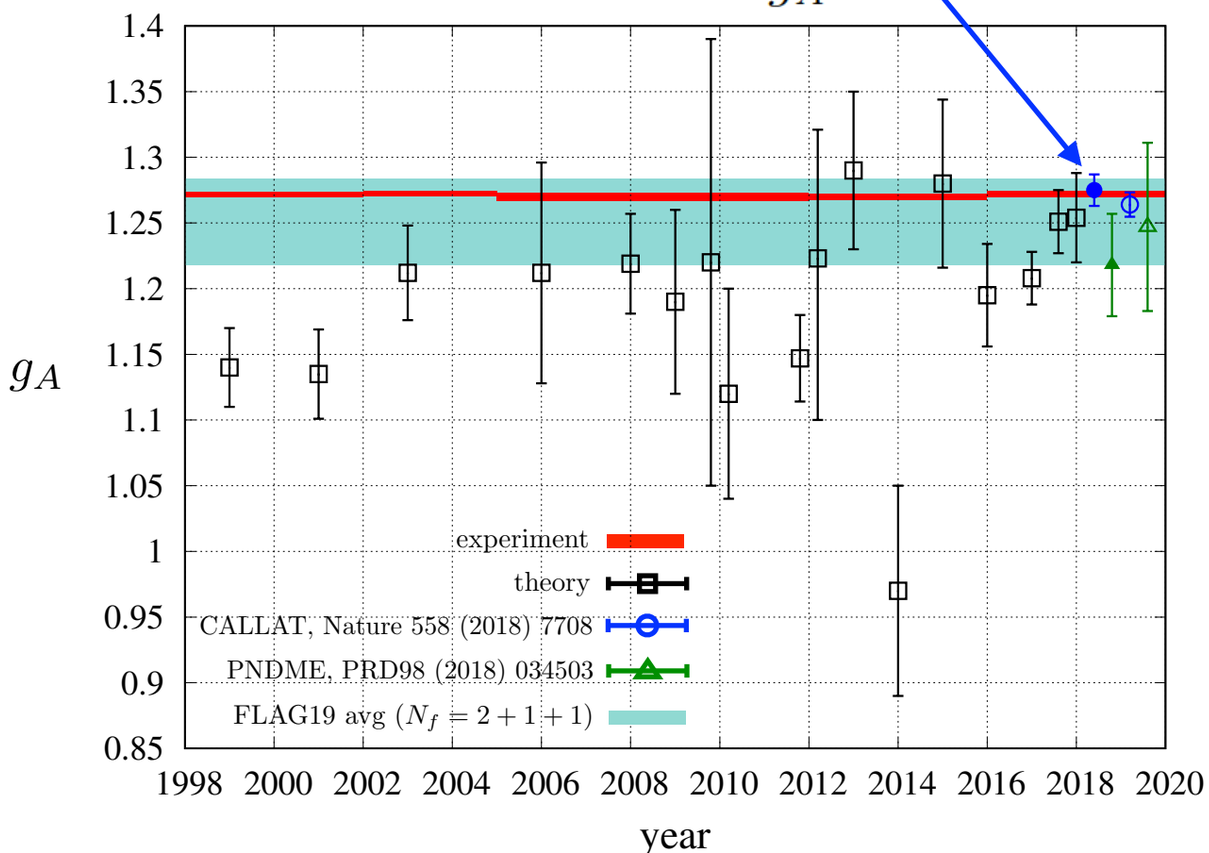

- Introduction
  - g_A and its phenomenology
  - experiment vs theory
- CalLat '18 calculation
  - simulation
    - HISQ 2+1+1 gauge fields
    - gradient flow smearing with Möbius DW valence quarks
  - Feynman-Hellmann Theorem inspired approach to correlators
  - renormalization; chiral, continuum, and infinite volume extrapolation
- Summary and outlook

Summary

LQCD will push g_A below 1% precision

- FLAG'19: $g_A = 1.251(33),\ 2.6\%$

CalLat precision possible due to...

- simulation (MDW on HISQ)
  - large statistics, range of m_q, inlcuding $m_q^{\rm phys}$, volume study
- gradient flow smearing with Möbius DW valence quarks
  - improved signal to noise, reduced discretization effects
- Feynman-Hellmann inspired correlators
  - improved signal to noise, control over excited states

Early Science time on Sierra and an INCITE award on Summit:

- improving g_A, calculating $F_{V,A}(q^2)$ and nucleon charge radii, ...

Bouchard et al, arXiv:1610.02354

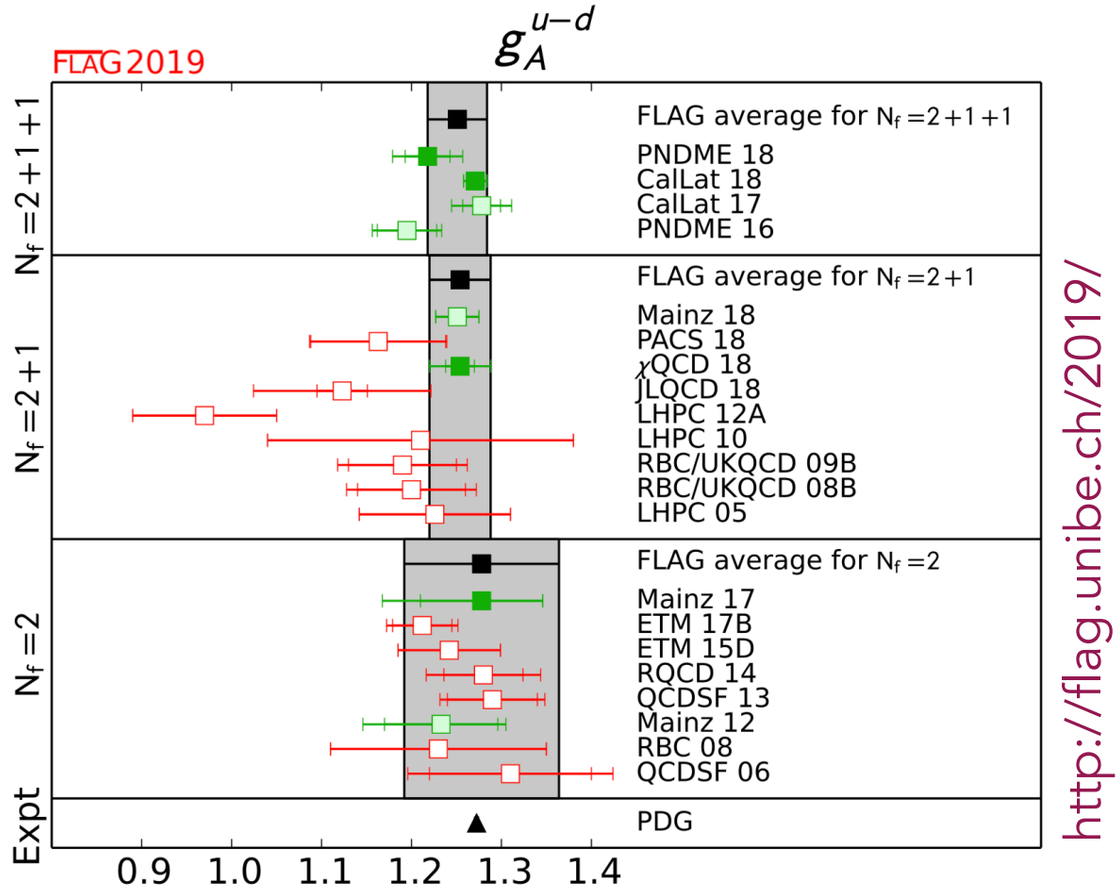

Outlook

CalLat, Nature 558 (2018) 7708

1 year on Titan (ORNL) + 2 years on GPU machines at LLNL

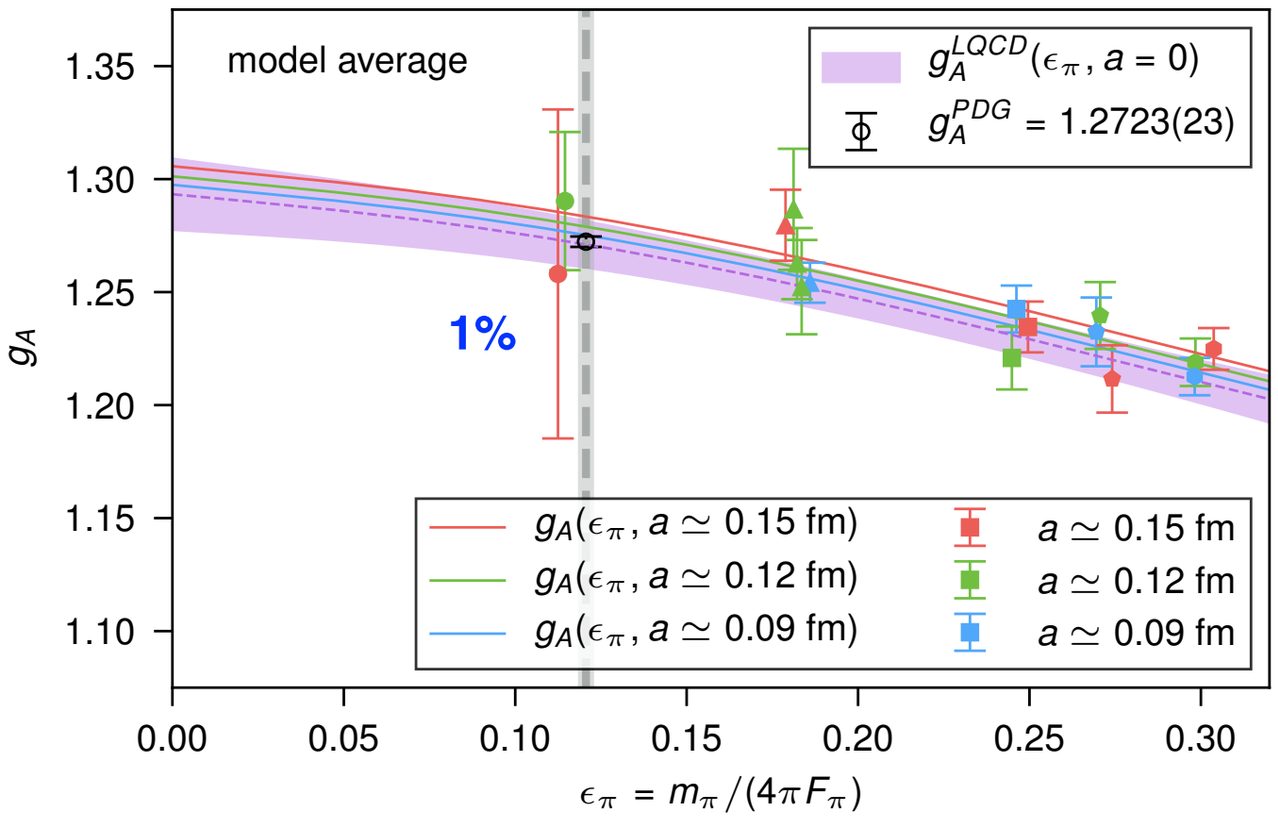

CalLat, PRELIMINARY

Sierra Early Science

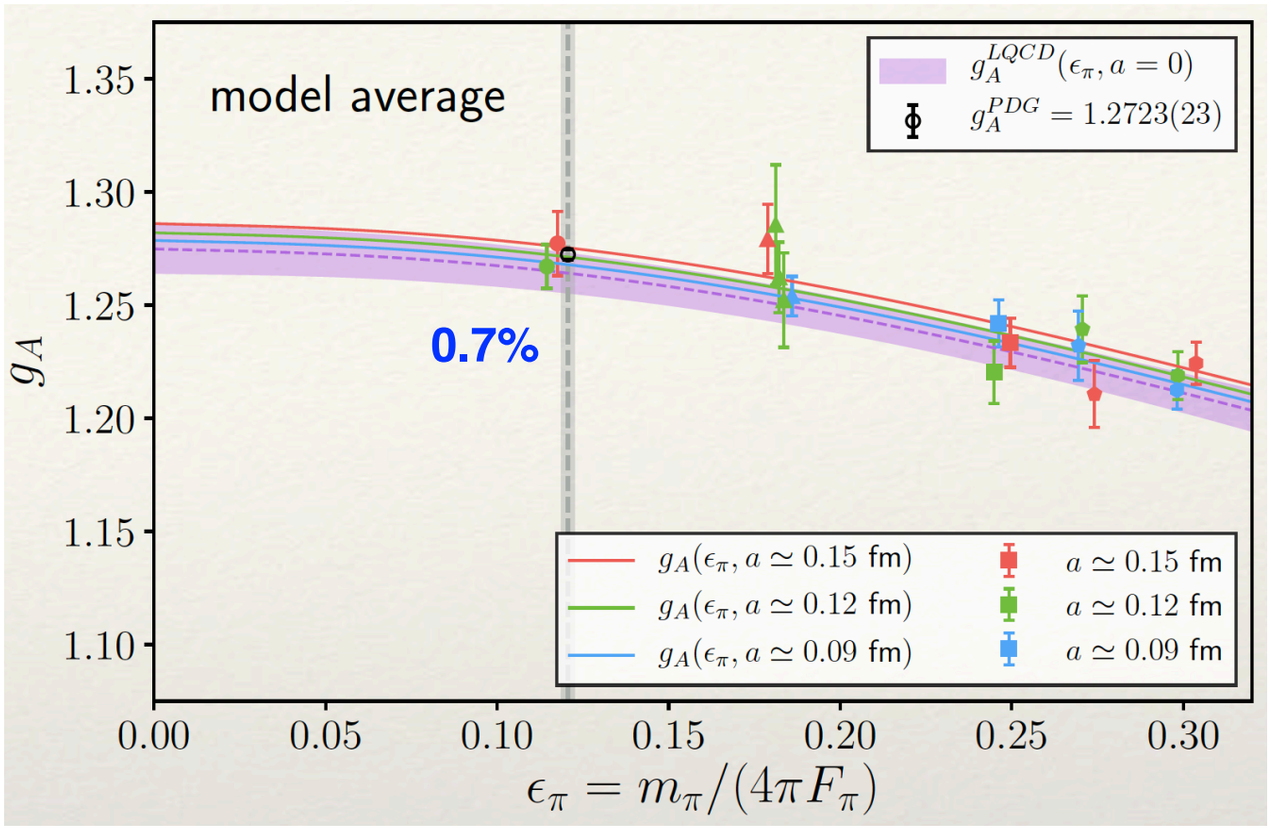

- vertical gray band denotes physical pion - significantly more expensive and valuable
- green point in Nature cost as much computing time as all others combined
- green point from Sierra has **10x** more statistics
- red point from Nature not useful
- red point from Sierra came from an entirely new calculation and is now very useful
- running on **Summit** with INCITE award (g_A,$F_{V,A}(q^2)$, charge radii, ...)

preliminary 0.7%, expect to reach 0.5%

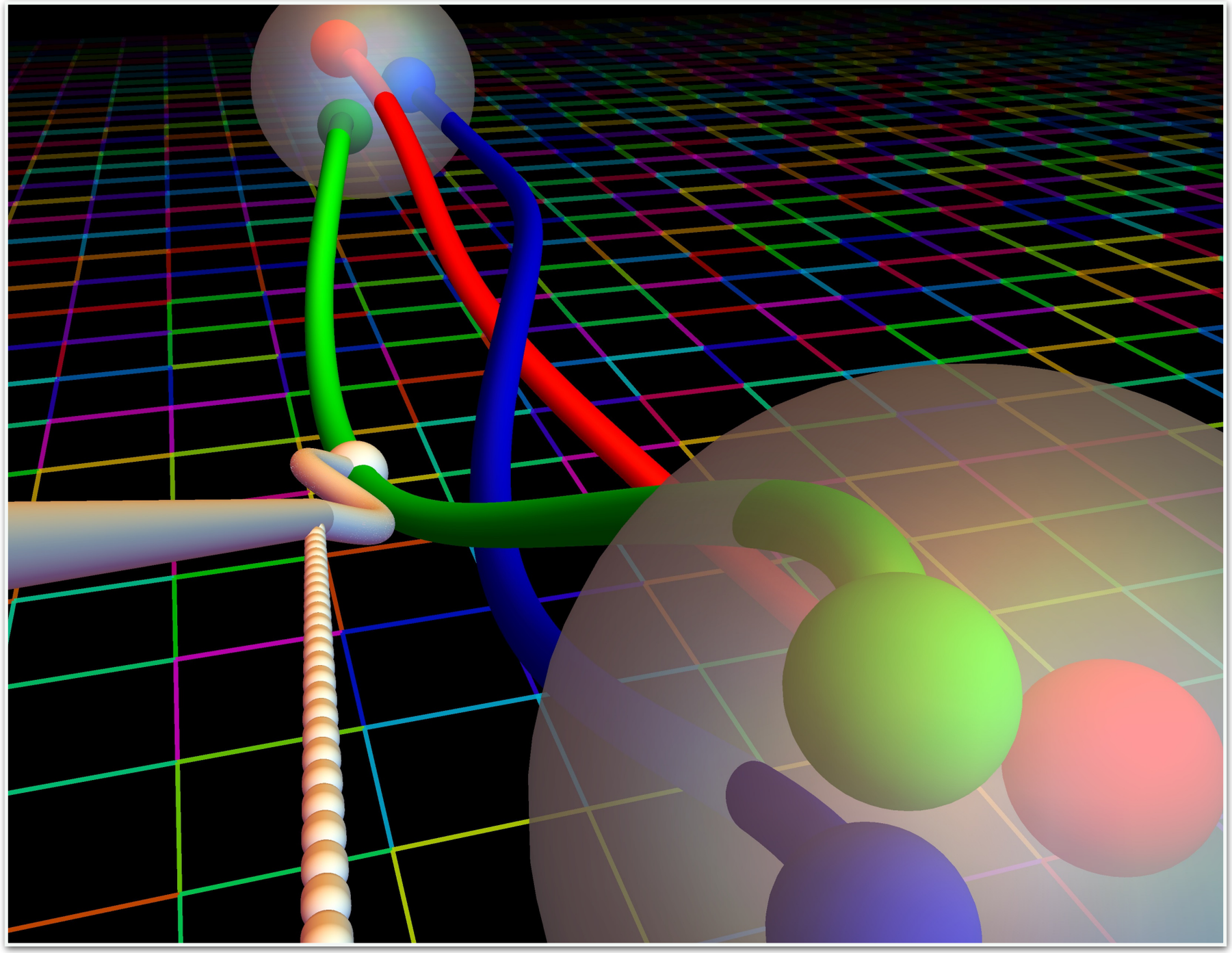

backup slides...

No sign of autocorrelations

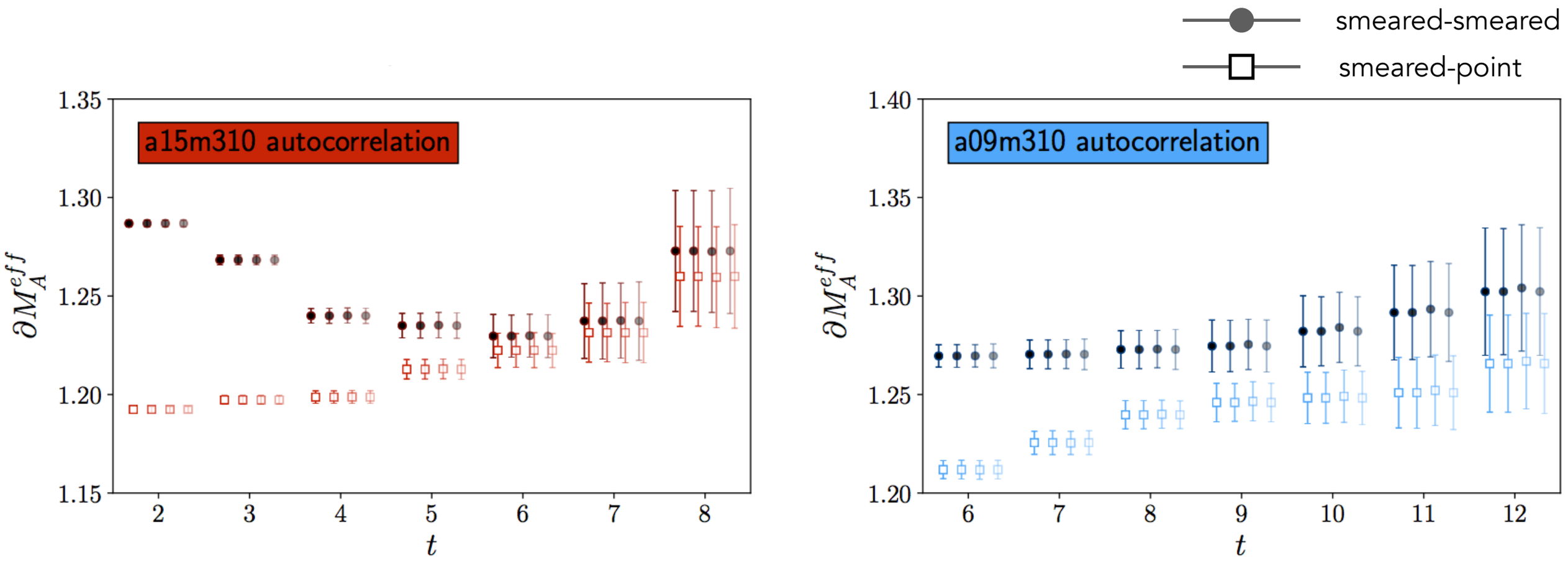

- at each timeslice, bin size = {1, 2, 3, 4}
- no change in uncertainties with bin size ⇒ no autocorrelations

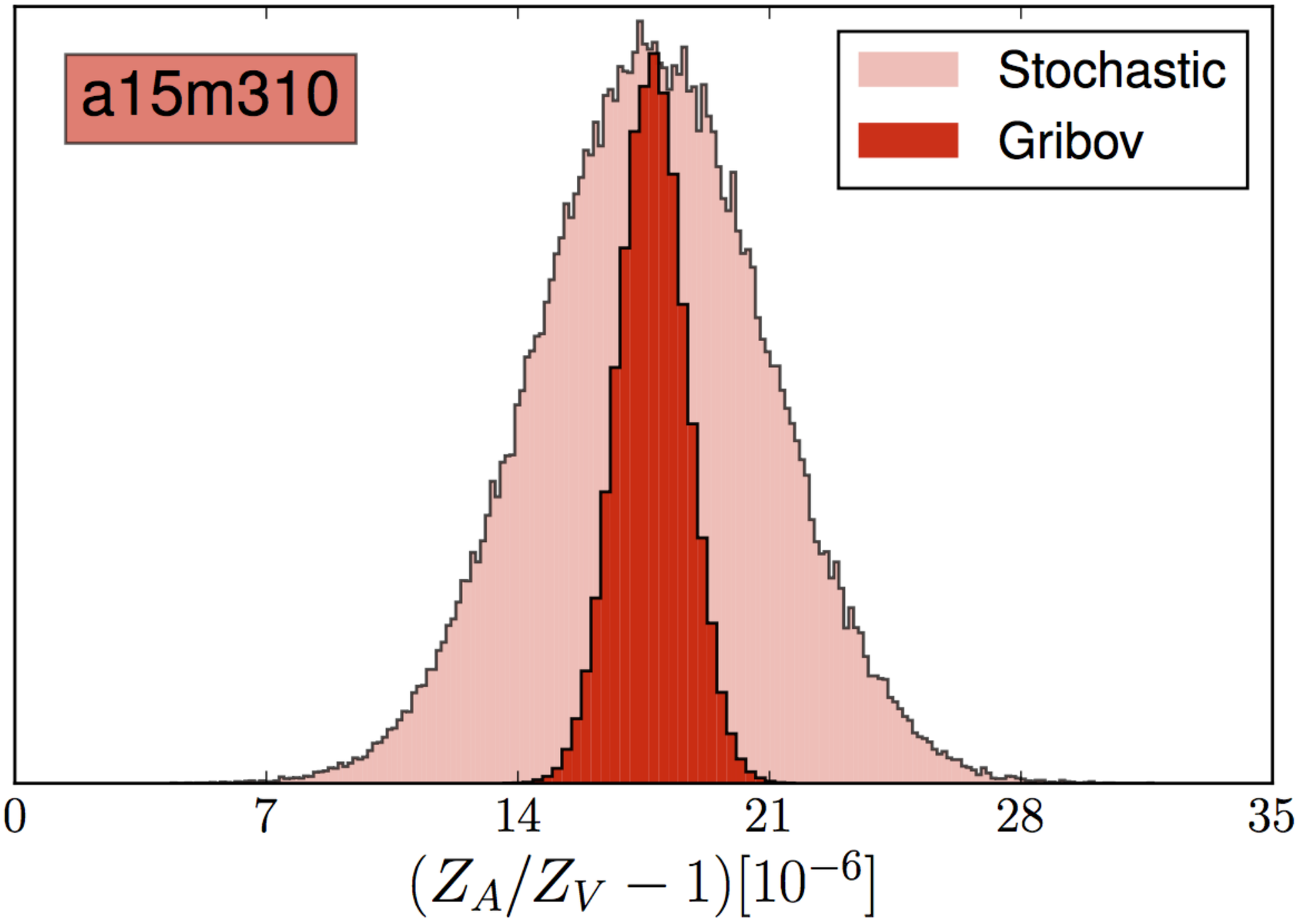
a15m310
Stochastic
Gribov
0
7
14
21
28
35
$(Z_A/Z_V - 1)[10^{-6}]$

Tuning valence MDWF to HISQ action

- for $t_{gf} = 1$
- fix L_5; optimize M_5 to minimize $m_{l,\,s}^{res}$
- vary b_5 to miminize L_5, while keeping $m_{l,\,s}^{res} \leq 0.1 m_{l,\,s}^{\mathrm{DW}}$
- tune $m_{l,\,s}^{\mathrm{DW}}$ s.t. $M_{\pi,\,s\bar{s}}^{\mathrm{DW}} = M_{\pi,\,s\bar{s}}^{\mathrm{HISQ}-5} \pm 2\%$
- vary t_{gf} keeping tuned parameters fixed

(Möbius) Domain Wall valence quarks

Kaplan, PLB 288, 342 (1992)
Shamir, NPB 406, 90 (1993)
Furman and Shamir, NPB 439, 54 (1995)

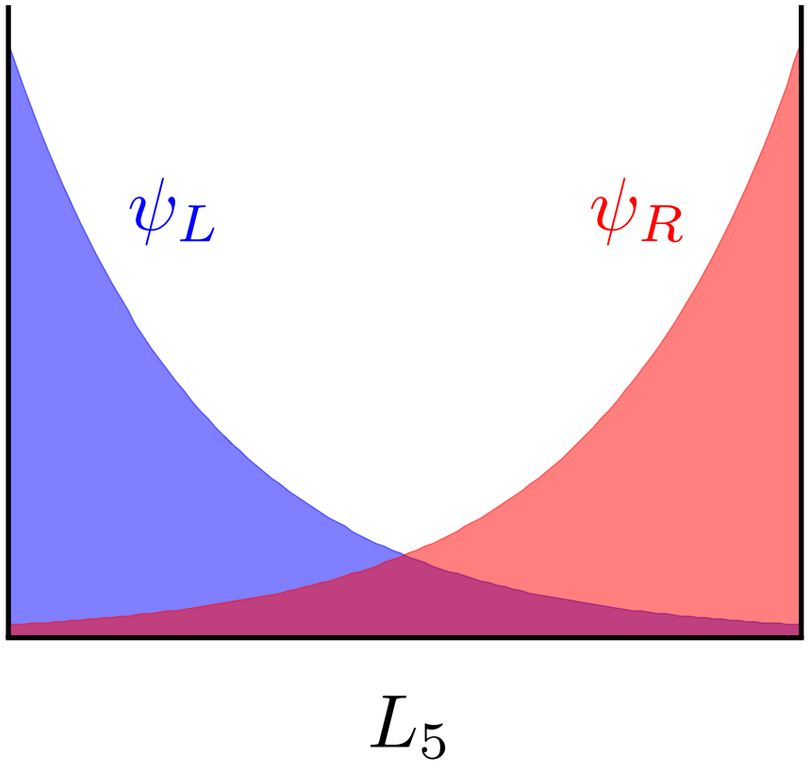

- modified chiral rotation

$$\delta\psi = i\epsilon\gamma_5\left(1 - \frac{D}{M_5}\right)\psi; \quad \delta\bar{\psi} = i\epsilon\bar{\psi}\gamma_5$$

- $\gamma_5 D$ generates translations in 5th dim
- Möbius is an implementation of D

Brower, Neff, Orginos, Nucl. Phys. Proc. Suppl. 140, 686 (2005)
Brower, Neff, Orginos, Nucl. Phys. Proc. Suppl. 153, 191 (2006)
Brower, Neff, Orginos, arXiv:1206.5214 (2012)

- residual chiral symmetry breaking, $m^{res} \sim \mathrm{overlap}(\psi_L, \psi_R)$
- discretization effects $\mathcal{O}(a^2)$
- we tune valence pseudoscalar masses = HISQ masses ± 2%

(Möbius) Domain Wall valence quarks

- multiple sources per configuration
- two combinations of sink-source Gaussian smearing
  - smeared-smeared
  - point-smeared

HISQ gauge configuration parameters							valence parameters							
abbr.	N_{cfg}	volume	$\sim a$ [fm]	m_l/m_s	$\sim m_{\pi_5}$ [MeV]	$\sim m_{\pi_5} L$	N_{src}	L_5/a	aM_5	b_5	c_5	$am_l^{\text{val.}}$	σ_{smr}	N_{smr}
a15m400	1000	$16^3 \times 48$	0.15	0.334	400	4.8	8	12	1.3	1.5	0.5	0.0278	3.0	30
a15m350	1000	$16^3 \times 48$	0.15	0.255	350	4.2	16	12	1.3	1.5	0.5	0.0206	3.0	30
a15m310	1960	$16^3 \times 48$	0.15	0.2	310	3.8	24	12	1.3	1.5	0.5	0.01580	4.2	60
a15m220	1000	$24^3 \times 48$	0.15	0.1	220	4.0	12	16	1.3	1.75	0.75	0.00712	4.5	60
a15m130	1000	$32^3 \times 48$	0.15	0.036	130	3.2	5	24	1.3	2.25	1.25	0.00216	4.5	60
a12m400	1000	$24^3 \times 64$	0.12	0.334	400	5.8	8	8	1.2	1.25	0.25	0.02190	3.0	30
a12m350	1000	$24^3 \times 64$	0.12	0.255	350	5.1	8	8	1.2	1.25	0.25	0.01660	3.0	30
a12m310	1053	$24^3 \times 64$	0.12	0.2	310	4.5	8	8	1.2	1.25	0.25	0.01260	3.0	30
a12m220S	1000	$24^3 \times 64$	0.12	0.1	220	3.2	4	12	1.2	1.5	0.5	0.00600	6.0	90
a12m220	1000	$32^3 \times 64$	0.12	0.1	220	4.3	4	12	1.2	1.5	0.5	0.00600	6.0	90
a12m220L	1000	$40^3 \times 64$	0.12	0.1	220	5.4	4	12	1.2	1.5	0.5	0.00600	6.0	90
a12m130	1000	$48^3 \times 64$	0.12	0.036	130	3.9	3	20	1.2	2.0	1.0	0.00195	7.0	150
a09m400	1201	$32^3 \times 64$	0.09	0.335	400	5.8	8	6	1.1	1.25	0.25	0.0160	3.5	45
a09m350	1201	$32^3 \times 64$	0.09	0.255	350	5.1	8	6	1.1	1.25	0.25	0.0121	3.5	45
a09m310	784	$32^3 \times 96$	0.09	0.2	310	4.5	8	6	1.1	1.25	0.25	0.00951	7.5	167
a09m220	1001	$48^3 \times 96$	0.09	0.1	220	4.7	6	8	1.1	1.25	0.25	0.00449	8.0	150

Gradient flow smearing

Narayanan and Neuberger, JHEP 03, 064 (2006)
Luscher and Weisz, JHEP 02, 051 (2011)
Luscher, JHEP 04, 123 (2013)

- begin with 4d gauge fields $A_\mu(x)$
- extend to continuous 5th dimension, t, via $B_\mu(t,x)$ for all μ s.t.

$$B_\mu(0,x) = A_\mu(x)$$

- diffusion equation drives "flow" in t toward classical minimum

$$\partial_t B_\mu = D_\nu G_{\nu\mu}$$

- common for scale setting, e.g., for $E = \frac{1}{4} B^a_{\mu\nu} B^a_{\mu\nu}$

$$\left(t\,\partial_t [t^2 E(t)]\right)\Big|_{t=w_0^2} = 0.3$$

- introduces length scale $l_{gf} \sim a\sqrt{8t}$ that smears out UV physics
- t will be t_{gf} throughout rest of talk

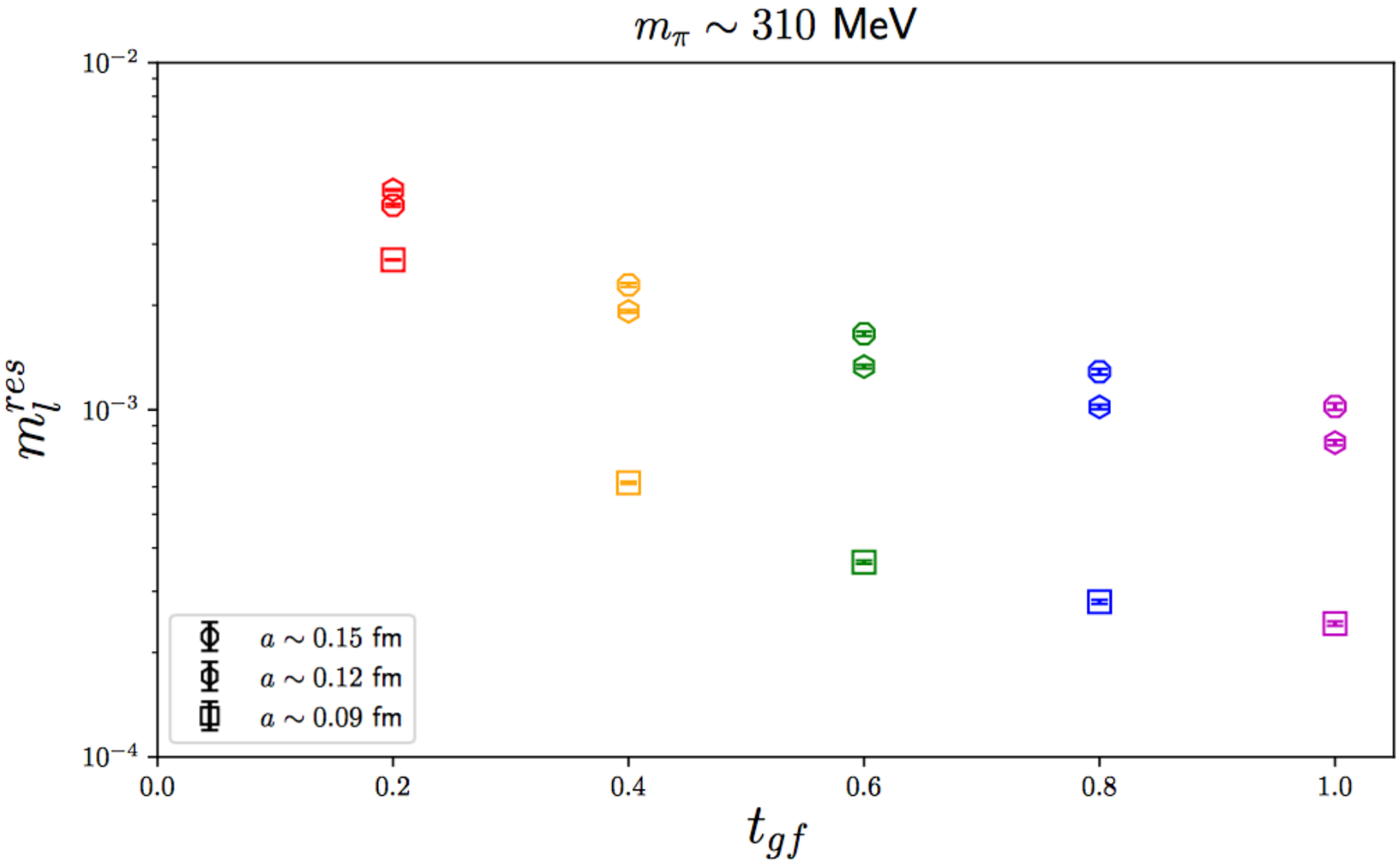

- residual chiral symmetry breaking reduced by smearing
- $m_q^{res} \leq 0.1 m_q$
- similar to DW on asqtad ensembles

Degrand, Hasenfratz, and Kovacs, PRD67 (2003) 054501

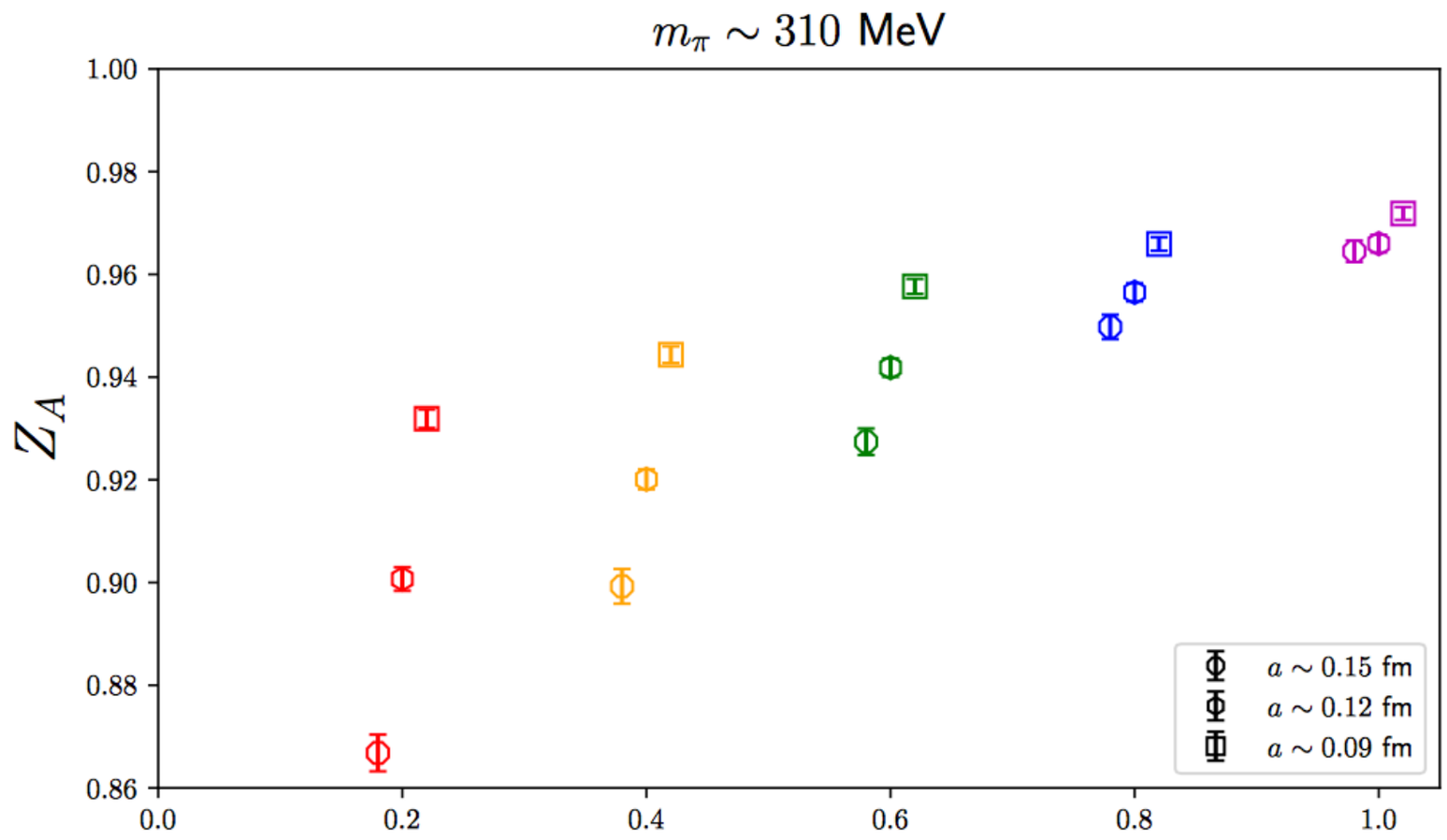

- g_V and g_A are obtained using currents

$$J_{V_4}(x) = \bar{q}^i_\alpha(x)\,\gamma_{4,\alpha\beta}\,\tau_3^{ij}\,q^j_\beta(x)$$

$$J_{A_3}(x) = \bar{q}^i_\alpha(x)\,\gamma_{3,\alpha\beta}\,\gamma_{5,\beta\gamma}\,\tau_3^{ij}\,q^j_\gamma(x)$$

- in chiral limit, J_{A_3} conserved and $Z_A = Z_V + \mathcal{O}(a^2) \sim 1$

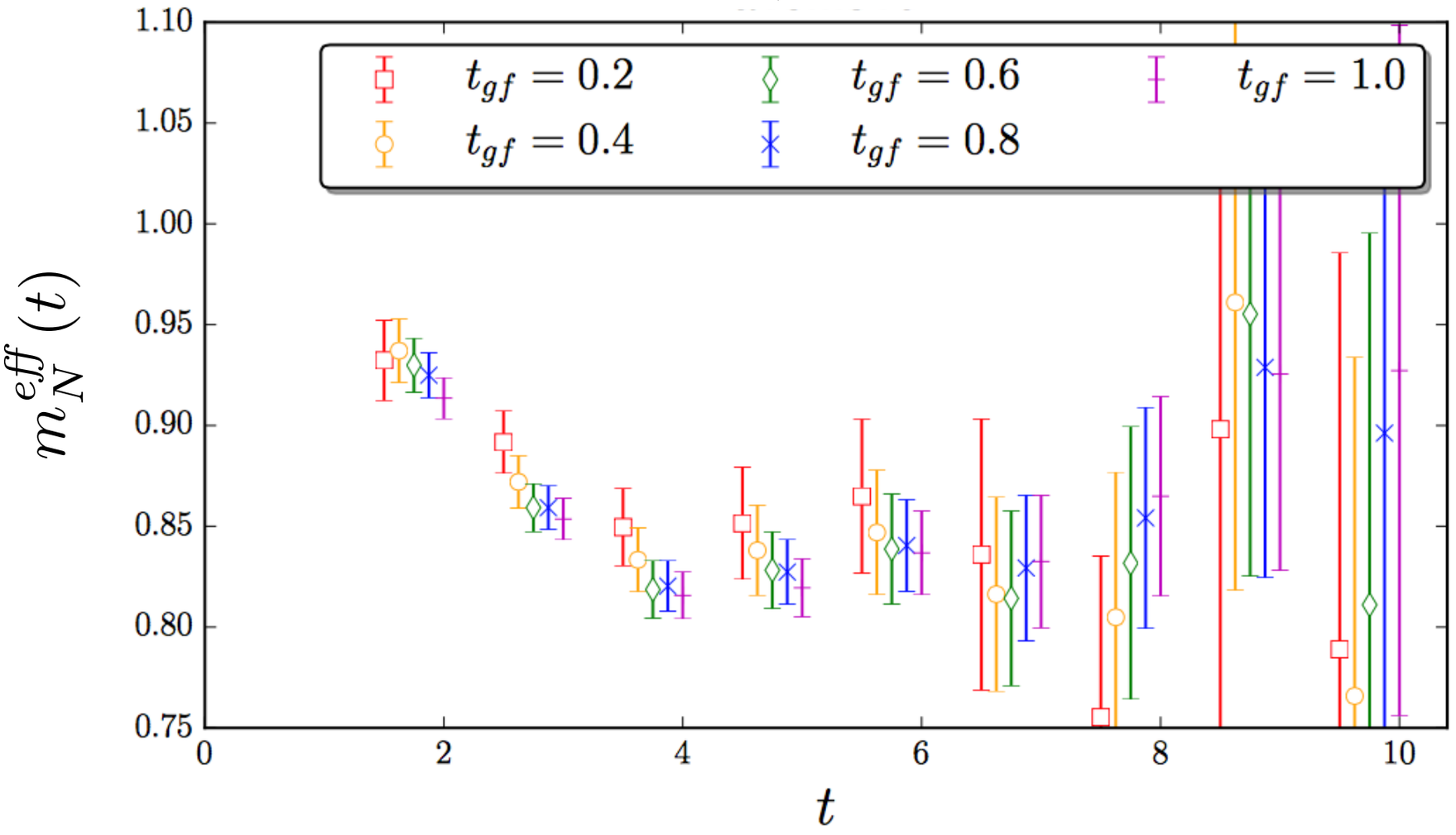

with increasing flowtime, we find:

- increased correlation between timeslices
- improved signal to noise, factor of $\sqrt{2}$ from fits

$m_N/F_\pi \quad (m_\pi \sim 310\ \text{MeV})$

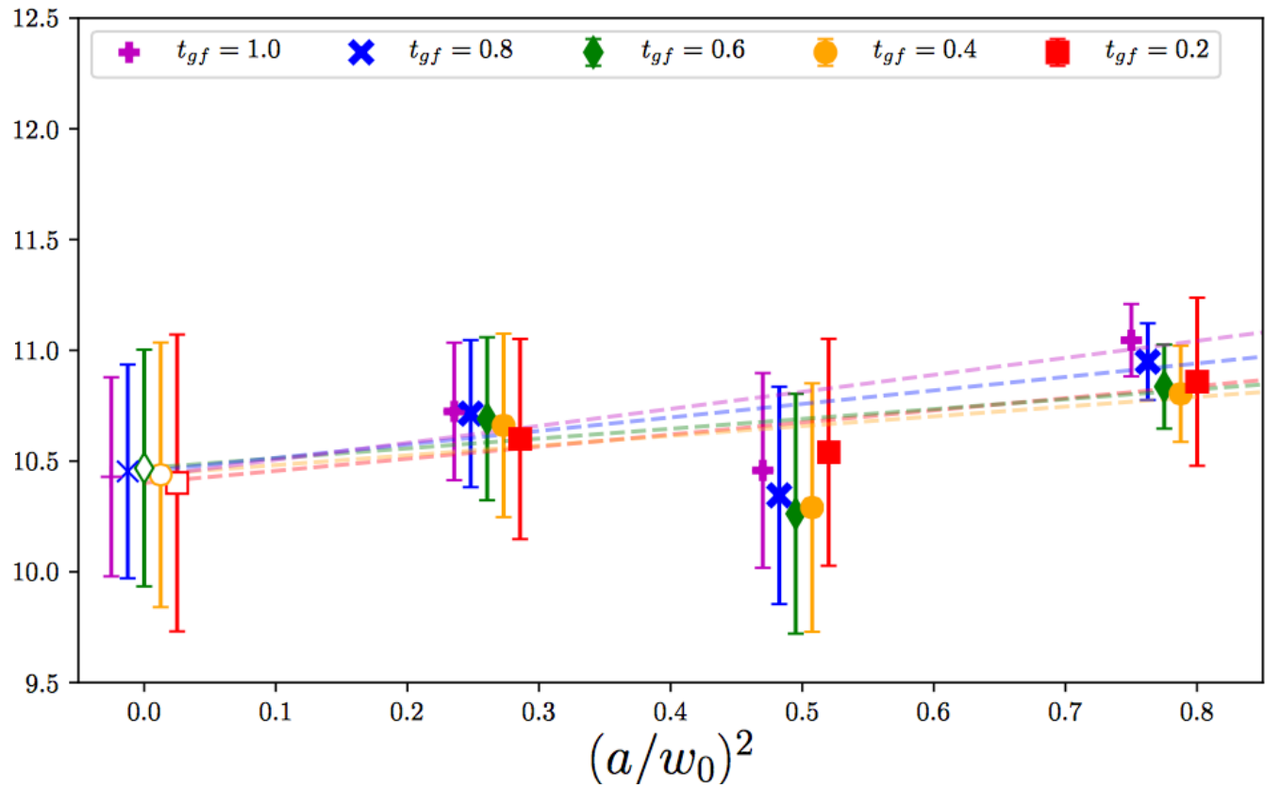

$F_{K\pm}/F_{\pi\pm}$

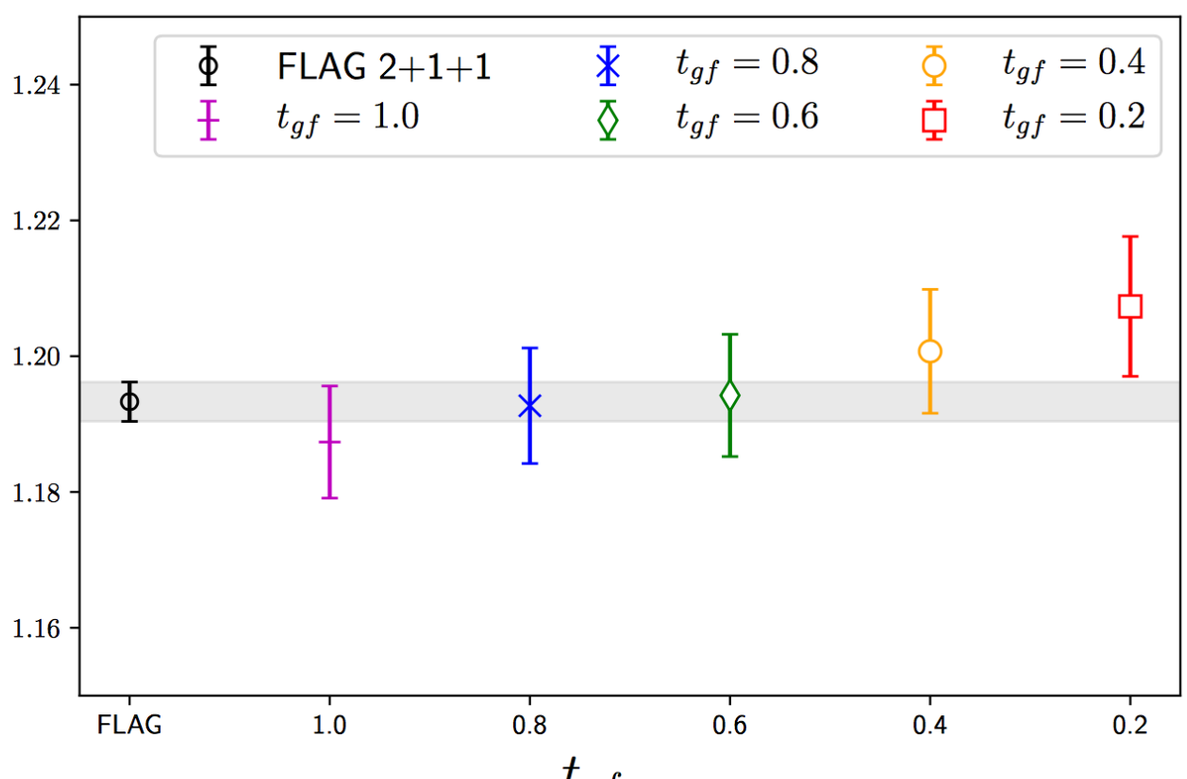

gradient flow as smearing results in:

- improved chiral symmetry $(m^{res},\ Z_A)$
- reduced discretization effects
- improved stochastic uncertainties
- continuum extrapolations independent of flowtime

correlator fit stability

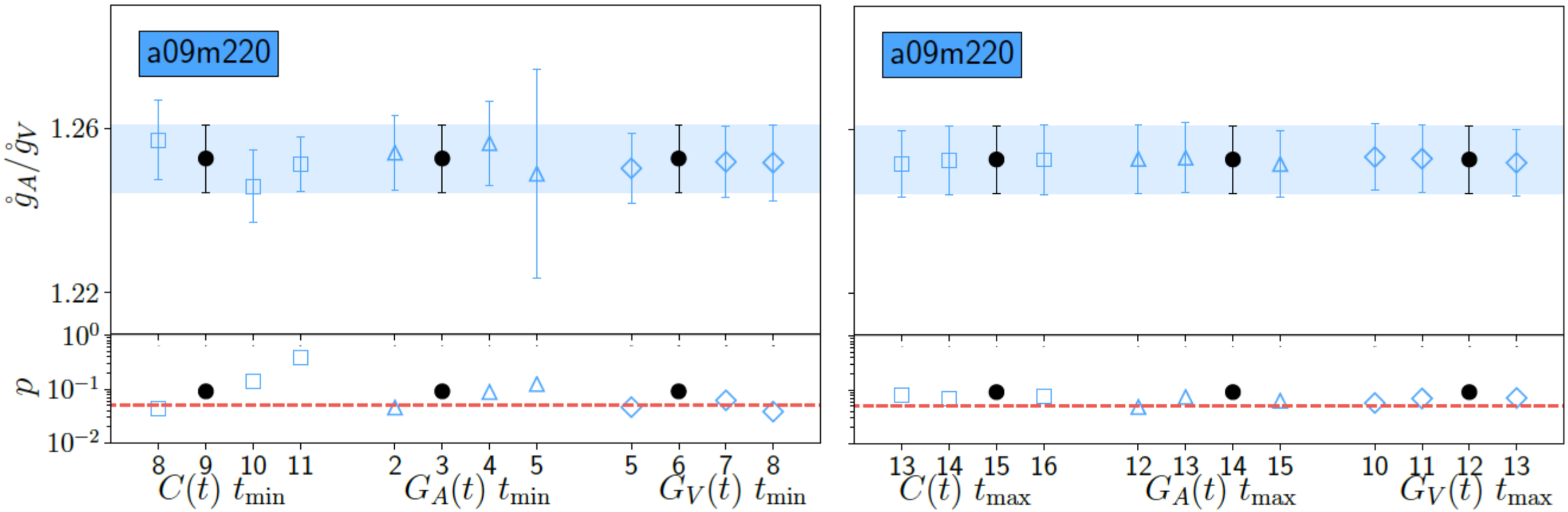

- study stability by varying
  - min/max timeslices included in 2pt correlator
  - min/max source-sink separation of FH correlator

Establishing convergence

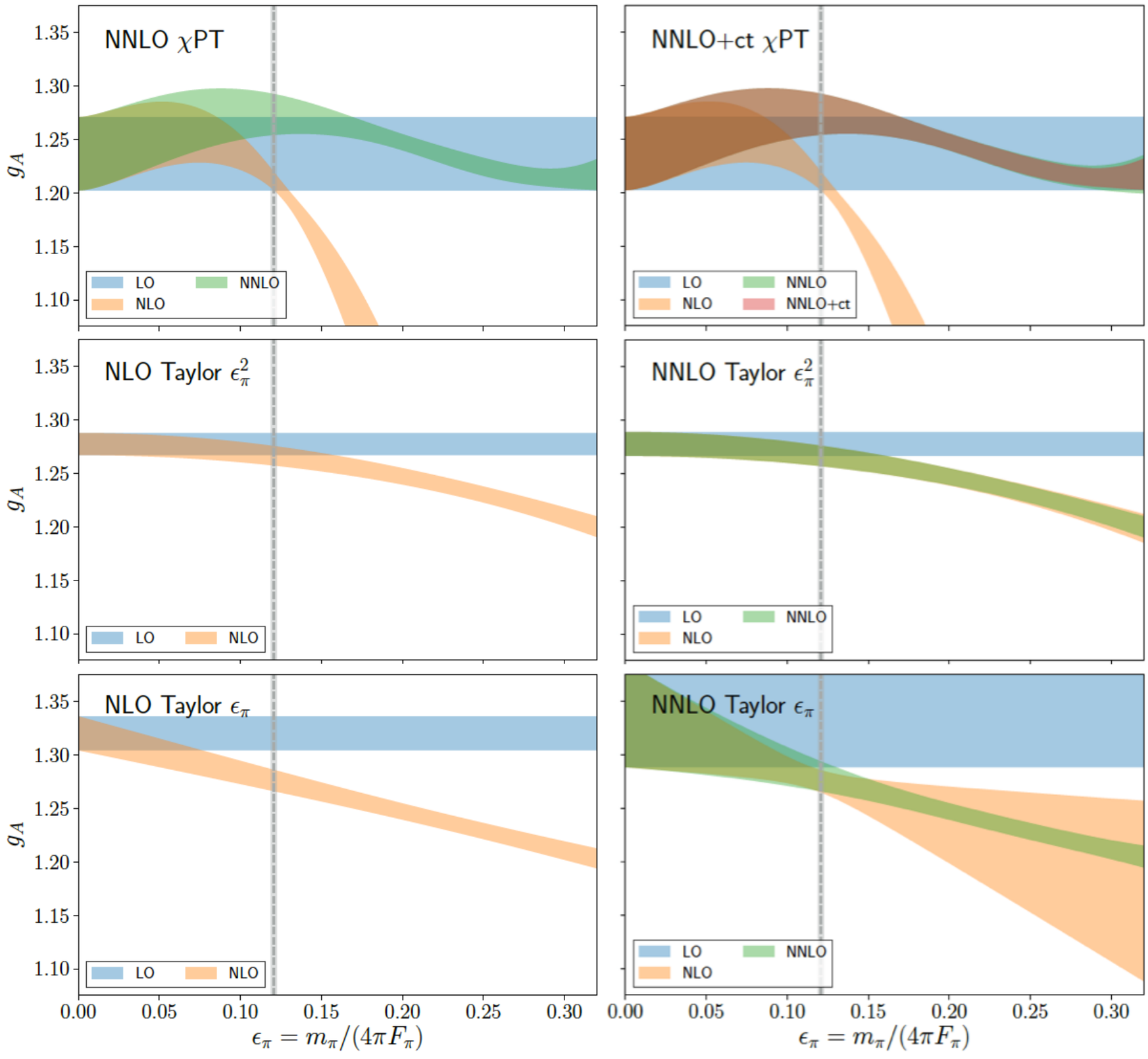

Effect of omitting lattice spacing data...

only 2 finest

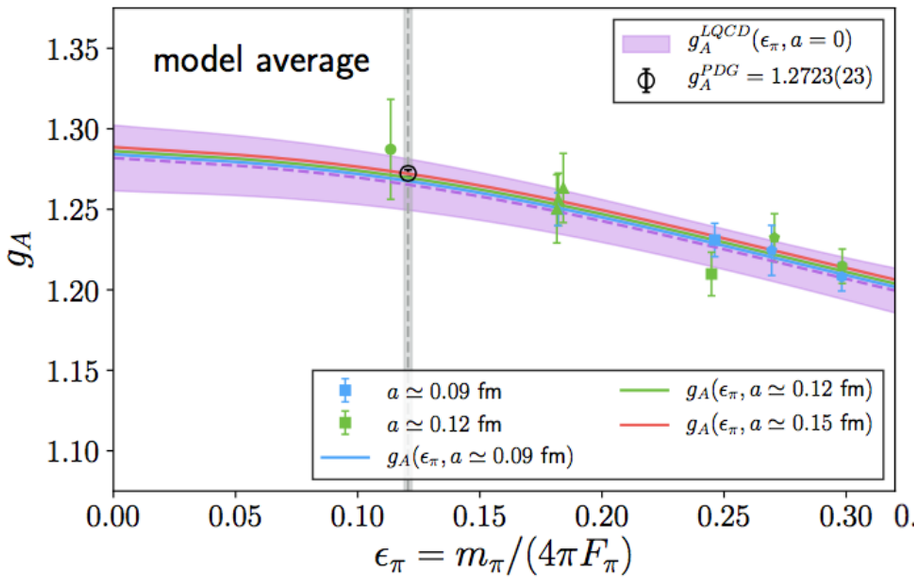

all

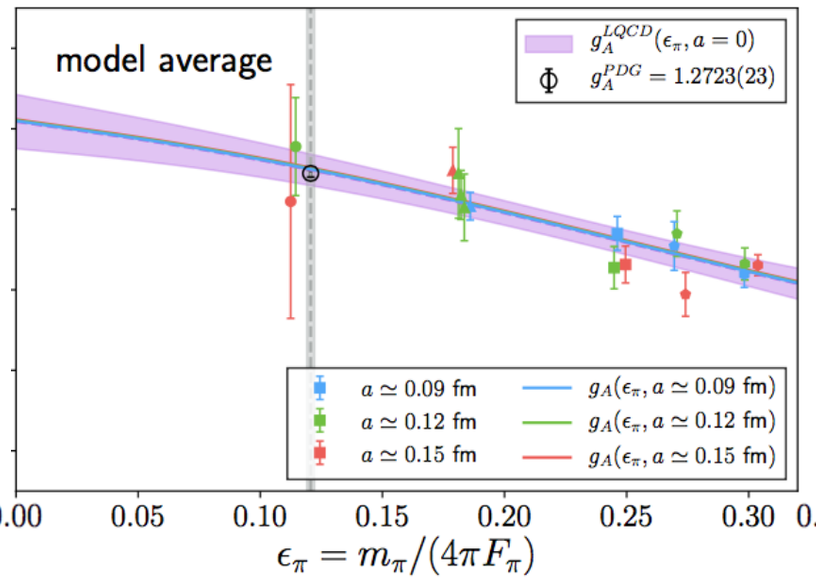

only 2 coarsest

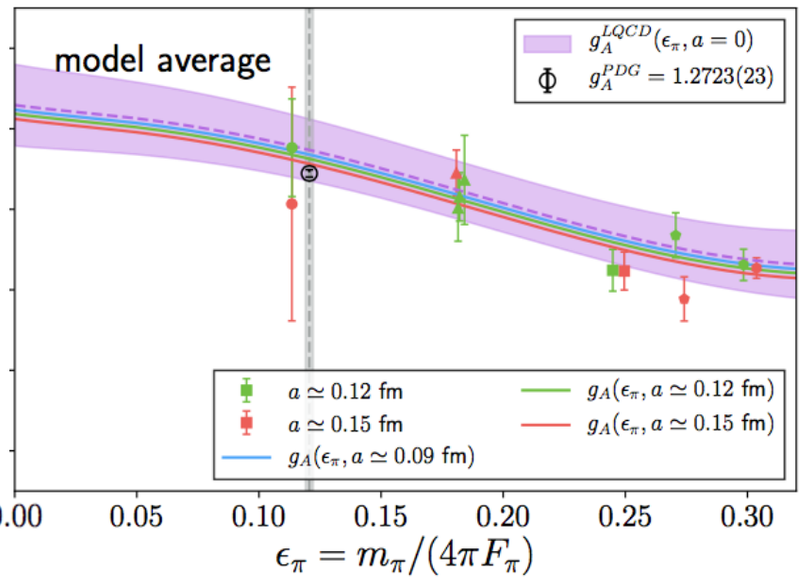

model average

$g_A^{LQCD}(\epsilon_\pi^{phys.}, \epsilon_a)$

Φ $g_A^{PDG} = 1.2723(23)$

$g_A(\epsilon_\pi^{(400)}, \epsilon_a)$

$g_A(\epsilon_\pi^{(350)}, \epsilon_a)$

$g_A(\epsilon_\pi^{(310)}, \epsilon_a)$

$g_A(\epsilon_\pi^{(220)}, \epsilon_a)$

$g_A(\epsilon_\pi^{(130)}, \epsilon_a)$

g_A

1.35
1.30
1.25
1.20
1.15
1.10

0.00 0.01 0.02 0.03 0.04 0.05 0.06

$\epsilon_a^2 = a^2/(4\pi w_0^2)$

model average

g_A

1.29

1.27

1.25

1.23

0.000

0.005

0.010

0.015

0.020

0.025

$e^{-m_\pi L}/(m_\pi L)^{1/2}$

NLO χPT prediction

ensemble	ϵ_π	$m_\pi L$	a/w_0	α_S	g_A
a15m400	0.30374(53)	4.8451(49)	0.8804(3)	0.58801	1.216(06)
a15m350	0.27411(50)	4.2359(47)	0.8804(3)	0.58801	1.198(13)
a15m310	0.24957(36)	3.7772(48)	0.8804(3)	0.58801	1.215(12)
a15m220	0.18084(30)	3.9673(45)	0.8804(3)	0.58801	1.274(14)
a15m130	0.11340(74)	3.227(19)	0.8804(3)	0.58801	1.270(72)
a12m400	0.29841(52)	5.8428(39)	0.7036(5)	0.53796	1.217(10)
a12m350	0.27063(69)	5.1352(49)	0.7036(5)	0.53796	1.236(14)
a12m310	0.24485(50)	4.5282(41)	0.7036(5)	0.53796	1.214(13)
a12m220S	0.18419(57)	3.2523(76)	0.7036(5)	0.53796	1.272(28)
a12m220	0.18221(42)	4.2959(56)	0.7036(5)	0.53796	1.259(15)
a12m220L	0.18156(44)	5.3604(61)	0.7036(5)	0.53796	1.252(21)
a12m130	0.11347(50)	3.899(12)	0.7036(5)	0.53796	1.292(30)
a09m400	0.29818(53)	5.7965(46)	0.5105(3)	0.43356	1.210(08)
a09m350	0.26949(57)	5.0502(62)	0.5105(3)	0.43356	1.228(15)
a09m310	0.24619(44)	4.5035(38)	0.5105(3)	0.43356	1.236(11)
a09m220	0.18197(37)	4.6990(32)	0.5105(3)	0.43356	1.253(09)

Stability of model average